ON-LINE FAILURE DETECTION AND DAMPING MEASUREMENT OF AEROSPACE STRUCTURES BY RANDOM DECREMENT SIGNATURES

NIELSEN ENGINEERING AND RESEARCH, INC.,
MOUNTAIN VIEW, CALIF

MAR 1973

1. Report No. NASA CR-2205	2. Government Accession No.	3. Recipient's Catalog No.
4. Title and Subtitle "On-Line Failure Detection and Damping Measurement of Aerospace Structures by Random Decrement Signatures"		5. Report Date March 1973
		6. Performing Organization Code
7. Author(s) Henry A. Cole, Jr.		8. Performing Organization Report No.
		10. Work Unit No.
9. Performing Organization Name and Address Nielsen Engineering and Research, Inc. 850 Maude Avenue Mountain View, California 94040		
		11. Contract or Grant No. NAS 2-6824
		13. Type of Report and Period Covered Contractor Report
12. Sponsoring Agency Name and Address National Aeronautics & Space Administration Washington, D.C. 20546		
		14. Sponsoring Agency Code

15. Supplementary Notes

16. Abstract

Random decrement signatures of structures vibrating in a random environment are studied through use of computer-generated and experimental data. Statistical properties obtained indicate that these signatures are stable in form and scale and hence, should have wide application in on-line failure detection and damping measurement. On-line procedures are described and equations for estimating record-length requirements to obtain signatures of a prescribed precision are given.

17. Key Words (Suggested by Author(s)) Failure Detection Damping Structures Random Vibrations	18. Distribution Statement Unclassified-Unlimited		
19. Security Classif. (of this report) Unclassified	20. Security Classif. (of this page) Unclassified	21. No. of Pages	22. Price*

TABLE OF CONTENTS

PRECEDING PAGE BLANK NOT FILMED

ON-LINE FAILURE DETECTION AND DAMPING MEASUREMENT OF
AEROSPACE STRUCTURES BY RANDOM DECREMENT SIGNATURES

By Henry A. Cole, Jr.
Nielsen Engineering & Research, Inc.

SUMMARY

Random decrement signatures of structures vibrating in a random environment are studied through use of computer-generated and experimental data. Statistical properties obtained indicate that these signatures are stable in form and scale and hence, should have wide application in on-line failure detection and damping measurement. On-line procedures are described and equations for estimating record-length requirements to obtain signatures of a prescribed precision are given.

INTRODUCTION

The risk of total failure of an aerospace structure is usually kept small by frequent inspections, but the cost is high[1] and use of the vehicle is lost during the inspection period (ref. 1). This may be particularly critical during the initial debugging period in which a failure in a single vehicle may cause grounding of an entire fleet and create bottle-necking in the inspection process. Much of the problem could be resolved if an onboard warning system could be developed which could detect incipient failures and indicate an individual inspection time for each vehicle. However, for such a system to be effective, it would have to avoid false warnings which might lead to unnecessary inspections and loss of operational capability.

The question is "How could flaws in the structure be detected when the vehicle is in service?" Visual inspection is obviously too incomplete without access to critical structural areas. Monitoring of acoustic emissions may be a possibility, but ambient noise sources are often so large that it would be difficult to detect the additional noise emanating from a small flaw. Another possibility is to analyze the structural

---

[1]Cost of inspection and repair of fatigue cracks alone in lifetime of a commercial airliner is of same order of magnitude as initial cost.

1

vibrations themselves and to look for changes in vibration characteristics. For example, in reference 2, the autocorrelation function of random vibrations was observed to change with the development of a fatigue crack in the structure, see figure 1. Unfortunately, the autocorrelation function also changes with variations in the random environment and false warnings of failure would be a problem under in-service operating conditions. Theoretically, the problem of changes of the signature due to changes in the input environment could be overcome by measuring both the input forces and the output vibrations and calculating cross-spectra or cross-correlations as described in references 3 and 4, but this is extremely difficult to do in practice because the input forces occur at so many points that they are almost impossible to measure. The problems with spectral and correlation methods are further complicated if the structure has nonlinear damping with amplitude which is often the case (ref. 2).

From the above it should be apparent that adaptation of methods which work under controlled or "laboratory" conditions to "in-service" conditions presents the difficult problem of distinguishing between changes caused by normal environmental effects and those due to flaws. Progress in solving this problem was reported in reference 2 in which variations in autocorrelation signatures were reduced by cross-correlation of the output signal with a stratified output signal. The results led to development of the random decrement method which is the subject of the present report. In this method, reference 5, segments of a random time history which start at a constant amplitude are selected by logic circuits and are averaged to form a curve which is called a "randomdec signature". To implement the method, a high-speed digital computer was built at Ames Research Center (ref. 6), and applied to a wind-tunnel wing model which was tested to destruction. Results indicated that the random decrement signature remained relatively invariant until an incipient failure occurred in the wing at which time the signature underwent significant changes which could be used in a failure detection system.

Another aspect of the use of randomdec signatures is in the measurement of damping which has applications in flight and wind-tunnel flutter tests and in prediction of response of structural modes. Damping is obtained in the same way as from a free vibration decay since the randomdec signature is representative of the free vibration decay curve which would

be obtained if the point on the structure were displaced to the selected amplitude and suddenly let go. For single-degree-of-freedom linear systems excited by white noise, the randomdec signature is identical in form to the autocorrelation function, but for multi-degree-of-freedom systems and non-linear systems, it differs in that the troublesome cross products (i.e., off-resonant vibrations mentioned in ref. 7) are absent. This should greatly simplify the separation of modes which occur at nearly the same natural frequencies and allow use of methods such as reference 8 rather than the more complicated procedure of reference 7.

Practical application of any signature method requires a knowledge of the precision of the signature for a given record length. To establish this for randomdec, a digital computer program was written which generated random time history responses of a specified mathematical model and then calculated the randomdec signature including its variance. These results have been analyzed and presented in the present report to show how the random decrement method can be applied in practical problems of failure detection and damping measurement.

<div align="center">LIST OF SYMBOLS</div>

AVG   signature with an initial displacement and a positive slope (see fig. 23)

AVH   signature with an initial displacement and a negative slope (see fig. 23)

AVT   randomdec signature obtained by averaging AVG and AVH

C_1 amplitude of signature at $\tau = 0$ due to distortion of input or filtering (see fig. 20)

C_2 amplitude of signature at $\tau = 0$ due to structural motion (see fig. 20)

f   frequency, Hz

f_n undamped natural frequency of a structural mode, Hz

$G(Q)$ value of time history Q time units after $y = y_s$ with a positive slope (see fig. 23)

$G(f)$ spectral density (defined on fig. 2)

$\overline{G}_H$ linear regression of $G(16)$ with constant H

$H(Q)$	value of time history Q time units after $y = y_s$ with a negative slope (see fig. 23)
$\bar{H}_G$	linear regression of $H(16)$ with constant G
K	number of peaks encountered for a selection level, y_s
M	number of digital points in a time history
N	number of individual segments used in randomdec signature (figs. 2 and 3) or number of cycles on signature used to calculate ζ on figure 12
P	period of oscillation, time units
Q	number of time units after $y = y_s$, abscissa of randomdec digital signatures
$R(\tau)$	autocorrelation signature defined on figure 2
r	correlation coefficient estimate
SR	sample rate, samples per second
T	record length, seconds
t	time, seconds
t_n	time for which $y = y_s$ numbered by subscript n (fig. 3)
$y(t)$	amplitude of time history at time t
$\bar{y}$	randomdec signature values from digital program
y_s	selection level
y_o	defined on figures 2 and 3
$\delta(\tau)$	randomdec signature defined on figure 2
ζ	damping ratio
ζ_{est}	damping ratio estimated from a signature
σ_F	rms of filtered time history
σ_o	rms of unfiltered time history
σ_y	rms of y

4

σ_r rms of random input

σ_ϵ standard deviation of randomdec signature at Q time units,

$$\sqrt{\frac{1}{2K}\left[\sum_{K=1}^{K} G_k^2(Q) + \sum_{K=1}^{K} H_k^2(Q)\right] - AVT^2(Q)}$$

τ time lag, Q/SR

ω frequency, radians per second

ω_n undamped natural frequency, radians per second

ω_1 frequency of filter half power point, 3 dB point, radians per second

INTERPRETATION OF THE RANDOMDEC SIGNATURE

In this section the basic concept of the randomdec signature will be developed as well as the intuitive reasoning which distinguishes the random decrement signature from other signatures. As was mentioned in the introduction, cross-correlation and cross-spectral methods which require measurement of the input forces are not considered to be practical under in-service conditions. Consequently, it will be assumed that the only measurement available is the output response of a strain gage or accelerometer located at a suitable point on the structure.

A typical random response of the transducer is shown on figure 2. Such responses are typical of in-service conditions of an aerospace structure in flight or during landing or takeoff on a runway. The random response curve itself is so complicated and variable that it cannot be used to detect changes although all of the information is contained within this time history. Various analyses may be performed on this curve to condense the information into a meaningful signature. One well-known technique shown on figure 2 is the spectral density which may be obtained directly from an ensemble average of the absolute amplitude squared of the Fourier transform of N segments of the time history. The resulting signature has a peak for each structural mode; and for well-separated peaks, the damping ratio of the mode may be obtained by measuring the width of the peak at half the peak value. This so-called bandwidth of

5

the half-power point is equal to $2\zeta f_n$. Also, the integral of the power spectral density is equal to the mean square value. Hence, the spectral density signature is useful in obtaining a broad picture of the frequencies of the structural modes, the energy in the modes and the approximate damping of isolated modes. However, the main problem of its use as a failure detector is that it is very dependent on the input as shown by the following equation from reference 4.

$$G_y(f) = |H(f)|^2 G_x(f)$$

in which $H(f)$ is the transfer function of the structure and $G_x(f)$ is the spectral density of the input forces. It may be seen that the amplitude and form of the output spectral density $G_y(f)$ are dependent on the amplitude and form of $G_x(f)$ which in our case is unknown. Hence, $G_y(f)$ is only truly representative of the structure if $G_x(f)$ is a constant (white noise).

Another dynamic signature shown on figure 2 is the autocorrelation which has been used extensively in on-line applications described in reference 2. For isolated modes, the signature has the same form as the free vibration decay curve of a structure with an initial displacement and may be interpreted as such to obtain period and damping of the mode. The autocorrelation is less sensitive than spectral density to variations in the spectral form of the input. In reference 2 the distortion of the signature due to the input is shown. The main problems with autocorrelation as a failure detector are that the level, $\overline{y^2}$, is dependent on the intensity of the input amplitudes and the signature will vary with the input if any nonlinear damping is present. The autocorrelation function may be used for measuring damping of isolated modes as was shown in reference 2, and for multi-mode applications in references 7 and 8.

The random decrement signature shown on figure 2 has an appearance similar to autocorrelation, but it has many properties which make it more useful as a failure detector. The first is that the signature has a constant amplitude, y_s, which represents a calibrated displacement of the structure. This is important because it fixes the level of the signature and makes it independent of changes in intensity of the input. Also, if the structure has nonlinear damping with amplitude, the fixing of amplitude stabilizes the form of the signature. Another property is that

6

the signature has the same dimensions as the original time history since
no multiplications are performed. Consequently, in multi-mode applications
troublesome cross products of modes are avoided; and in applications where
the input spectral density is not flat, the signature distortion is
considerably less. Other more subtle properties will become apparent in
later sections of the report.

Although the equation on figure 2 describes the process, a better
feel for the extraction of the signature is obtained by graphically
performing the process as shown on figure 3. First, the selection level,
y_s, is set. Each time the curve passes through $y_0(t) = 0$, a segment of
the curve is placed in summation. The first two segments are shown on
the figure, one with an initial condition of a plus slope and one with
an initial condition of a minus slope. The average of these two is the
signature $\delta(\tau)$ for $N = 2$. As more samples are taken, the signature
converges to a form as shown for $N = 100$. For a single-degree-of-freedom
system the value $\tau = P$ would be the period of oscillation. For this
particular value of τ, a histogram of the number of points at various
levels is shown. This tends to be normally distributed about $\delta(P)$, and
as will be shown in Appendix A the standard deviation, σ_ϵ, is small and is
almost independent of the damping ratio. In failure detection devices we
can use the standard deviation, σ_ϵ, to set a confidence level according to
the number of false alarms which we are willing to accept; and in damping
measurements we can use it to specify the record length needed to obtain
damping of a specified accuracy.

Another interesting aspect of the random decrement process is shown
on figure 3(b) which shows the distribution of time between the samples
selected. If the time history were a sine wave, the samples would be
taken periodically. For a narrow band process, such as shown here, the
samples are taken with a random distribution in time about the period of
the system. For a white noise time history, one might expect that samples
would be taken completely at random.

Now the question is "How is the signature related to the structure?"
A hypothesis for linear systems is shown on figure 4. This shows the
process as the linear superposition of a step, an impulse and random
response for each segment of the time history selected. In other words,
the step represents the homogeneous solution to an initial displacement,

the impulse represents the homogeneous solution to an initial velocity, and the random response represents the particular solution to random inputs which occur during the sample segment. It may be seen that all of the step responses are the same, whereas the impulse responses have initial slopes with alternate plus and minus values of varying magnitude. The random responses are of course random. When a large number of the segments are averaged, only the step response is left because the impulse and random responses tend to average to zero. If the inputs do not have a zero mean, then the signature obtained will still start at $y_0 = 0$ but will not end at $-y_s$. In other words, the signature will be for a loaded structure, and this must be taken into account in the interpretation (i.e., y_s should be selected as the deflection from the equilibrium position.) Of course, signatures could be obtained by taking only segments with an initial slope of a plus value, but then the signature would vary with intensity of the input amplitude.

For nonlinear systems, the superposition arguments cannot be used so that an exact interpretation of the relation of the signature to the structure cannot be made at present. It seems likely though that for small damping, the signature should be close to the free oscillation curve for the nonlinear system. For failure detection, the important thing is that the curve should be repeatable under various ambient conditions.

It is quite apparent that considerable work needs to be done in going backward from the signature to the mathematical equations which define the system. This is not the present purpose. The signatures do provide a check on the linearity of a system if multiple selection levels are used. Also with multiple selection levels, the multiple signatures which are obtained should provide a print which would uniquely identify the system and provide a standard for failure detection.

ON-LINE FAILURE DETECTION

From the foregoing section it was shown that the randomdec signature gives a curve which is related to the free vibration decay of the structure with an initial displacement. The scale and form of this curve is always the same even when the intensity of the ambient random forces changes in

contrast to spectral density and autocorrelation which vary with changes in the ambient random forces. In this section, the hypothesis and application of the method to failure detection is developed.

A typical experimental setup is shown on figure 5. It should be noted that although the spectral analyzer is not part of the failure detector, it still serves a purpose in providing a broad view of the location of structural modes which may be used as an aid to specifying filtering requirements. Let us consider now what happens to the signature when a fatigue crack develops in a structure. A fatigue crack introduces additional degrees of freedom which are excited by the random forces. When the crack is small, small blips would show up in the hashy, high-modal density region of the spectral density; in this form detection would be difficult. As the flaw grows, the frequency of the failure mode would be expected to decrease until it approaches the fundamental modes. By the time a flaw reaches the low-frequency range it would be so serious that it would either be obvious or complete failure would be imminent. To detect the failure mode it needs to be intercepted at a high enough frequency so that corrective action can be taken and complete failure avoided. To do this the random signal is passed through a band-pass filter which is set at a high frequency. With the undamaged structure, standard randomdec signatures are established for all loading conditions and environments. If a failure develops, it will have a powerful effect on the signature because it will dynamically couple with structural modes within the band-pass frequencies of the filter. For the failure detector, once the standards have been established only parts of the signature at peaks need to be calculated with warning devices sensitive to voltage changes in the peak values.

A procedure for failure detection is outlined on figure 6, which shows only a single peak for illustration. The standard signature region is first established to a confidence level consistent with percent of false alarms which could be tolerated. For the 95-percent confidence level shown, of course, false warnings would occur 5 percent of the time. Detection would be as shown on the figure. The check on standard deviation, σ_ϵ, is to prevent false indications due to extraneous input sources other than the normal random excitation, i.e., a sinusoidal force or signal in the electronics. For example, if a sinusoidal force were applied to the structure, the signature would become an undamped cosine wave and fall outside the standard region, but the standard deviation would fall to zero.

In this case the amber light would go on. In the on-line computer built
at Ames Research Center this check on σ_ϵ was not included and may not
be necessary unless a high level of reliability of the device is desired.

Experiment with Truss

Some laboratory experiments were conducted to check the sensitivity
of randomdec signatures. Figure 7(a) shows the experimental setup with a
truss structure with bolted joints. Figure 7(b) shows the spectral density
of the output of the accelerometer. The amplitudes were so small that they
could not be detected visually, but were apparent from the emitted sound
and fingertip feel. From the spectrum several frequency ranges were
selected as suggested on figure 5. Ranges where a distinct peak followed
by a distinct valley were selected since it was felt that these would
result in signatures with distinct peaks. The aim of the test was to see
if a difference between tight and loose bolts at joint A-B could be
detected. For the filter range 600-800 Hz, the spectral densities for
bolts tight and loose are shown on figure 7(c). The difficulty in dis-
tinguishing between the two curves is obvious. For the same data set,
the signature obtained from the randomdec computer is shown on figure 7(d)
and the change in the signature is readily apparent. Similarly, for the
frequency range 1100-1300 Hz (fig. 7(e)), the change in the randomdec
signature is apparent but not as distinct. This experiment was not
extensive, but it points to one of the key problems in failure detection.
That is, a particular frequency range and transducer location may be best
for detection of a particular flaw. Obviously, experience is needed with
different failure mechanisms in order to establish the standard signature
which should be used in the detection device.

Experiment with Flutter Model

Another example of failure detection with the randomdec computer was
reported in reference 6 for a wind-tunnel model undergoing flutter.
Instrumentation of the model consisted of strain gages at the root as
indicated on figure 8. Randomdec signatures taken at intervals are shown
for a frequency range above the natural frequencies of the first three
modes. For the first 2 minutes and 45 seconds the signatures fell within
the narrow range indicated by the "standard." The signature then underwent

10

a sequence of large changes until finally the wing failed and the signal stopped. It is apparent from this sequence that the randomdec signature was sensitive to an incipient failure in the wing which occurred a considerable time[2] before the wing failed completely. The changes in the signature are sufficiently large to enable a failure detector utilizing the voltage of a point on the second peak to anticipate the failure. The importance of selecting the proper frequency range is emphasized by figure 8(b) which shows the signatures obtained from the unfiltered time history. Although changes in the signature are apparent, the voltage changes are not sufficiently large to be used in a failure detector.

Figure 9 shows samples of the time history taken at the same times as the signature. This demonstrates the complexity of the original signal from which the signatures were obtained.

MEASUREMENT OF DAMPING

Damping measurements are important for prediction of structural response, definition of flutter boundaries, and detection of malfunctions of dampers in flight (i.e., stability augmentation systems, engine shock mounts, etc.). On-line monitoring of such systems could contribute to flight safety since there are many cases of accidents involving engine mount dampers. Also, if present-day proposals for systems to control flight flutter are implemented, on-line damping monitoring systems will be needed for flight safety.

On-Line Measurement

In flight and wind-tunnel flutter tests such as described in reference 2, damping values are needed as soon as possible. As shown in Appendix A, for a single-degree-of-freedom system the randomdec signature may be used directly to extract damping ratios. Of course, real systems always contain many modes and several techniques are followed to reduce the response to an effective single-degree-of-freedom system. These are discussed later in the section on experimental procedures. For the

---

[2]On a full-scale vehicle, warning time would have been 7-1/2 minutes.

present we will assume that the signal has been effectively reduced to that of a single-degree-of-freedom system. When this has been done, and no distortion is present due to filtering or spectral shape of the input, the damping ratio may be read directly on the oscilloscope by putting a damping ratio scale on the peak as shown on figure 10(a). Sometimes it is useful to set the scope sweep faster than the signature sweep as shown on figure 10(b) so that the beginning part of the signature also appears at the end of the signature. Small changes in damping and frequency may easily be detected by viewing this region.

Oftentimes, it is desirable to know if nonlinear effects with amplitude are present. This can be done on line by superimposing signatures with different selection levels as shown on figure 11. In the example shown the selection level of one signature is one half that of the other. To allow direct comparison of the signatures then, the 0.5v signature is multiplied by 2 in the display.

As is shown in Appendix A, the signatures are sometimes distorted by filtering and spectral variations of the input. When this occurs, damping ratio should be measured as shown on figure 12 which was obtained from the well-known equation:

$$\ln \frac{y_2}{y_1} = \frac{-2\pi N \zeta}{\sqrt{1 - \zeta^2}}$$

This process, although not a direct readout method, may be performed rapidly during a test and compensates for most severe distortion problems. If a Gerber variable scale is used, the y_2/y_1 ratio can be measured directly without performing the division.

A somewhat slower alternate method is shown on figure 13. This method may be used if time is available for plotting points and if an estimate of the distortion as in reference 2 is desired. The distortion usually occurs in the first two points so a straight line is faired ignoring these points. The equation for damping ratio shown on the figure is obtained by assuming $\sqrt{1 - \zeta^2}$ to be negligible and solving for ζ in the equation above. Thus

$$\zeta = \frac{\ln y_1 - \ln y_2}{2\pi N}$$

To convert the logarithms to a scalar measurement we multiply by $\ln 10/X_o$ in which X_o is the scalar length of one decade on the logarithm scale used. The equation becomes

$$\zeta = \frac{2.3026}{2\pi} \frac{X}{NX_o}$$

in which X is the scalar distance representing the difference in logarithms as shown in the example.

Several useful rule-of-thumb methods for obtaining damping ratio are:

$$\zeta \simeq \frac{y_1 - y_2}{2\pi}$$

for small ζ and $y_1 = 1$. Note that if a variable scale is used y_1 can be set to 1 and $y_1 - y_2$ measured directly. And

$$\zeta \simeq \frac{1}{9.08C_{1/2}}$$

where $C_{1/2}$ is the estimate of the number of cycles to half amplitude.

Off-Line Measurement

Usually random time histories are recorded on magnetic tape; and following a test, accurate values of damping are wanted for use in response prediction. Several examples of damping measurement were worked out on experimental data obtained by the Aeronautical Structures Branch at Ames Research Center from vibration of a 0.2286- by 0.3048-meter panel 0.00235-meter thick in a turbulent boundary layer at Mach numbers from 2.5 to 3.

Figure 14(a) shows the spectral density for an isolated mode obtained by Fast Fourier transform of 4098 points taken at a sample rate of 8000 samples per second. The difficulty of measuring damping by measuring the bandwidth of the half-power point is obvious. Figure 14(b) shows the randomdec signature for the same data set with damping measurements obtained by the method of figure 12. Note the consistent values of ζ_{est} for $N = 1, 2,$ and 3.

Using equation (A-8) in Appendix A at a confidence level of 95 percent, the fractional error is

$$F_\zeta = \frac{1.96}{\sqrt{(0.51)(4)(0.008)(771)}} = 0.55$$

Values of ζ measured on four such signatures were 0.007, 0.006, 0.007; 0.010, 0.011, 0.012; 0.007, 0.007, 0.007; and 0.009, 0.009, 0.009 which fall within the predicted range of 0.0083 ±0.0046. The consistency of values for $N = 1, 2,$ and 3 and the range of values lends confidence to the record length predictions for ideal single-degree-of-freedom systems which were obtained in Appendix A.

Figure 15(a) shows the spectral density of two modes which could not be separated by filtering without excessive distortion of the signature. The randomdec signature is shown on figure 15(b) and it may be seen that the values of ζ_{est} are increasing with N which indicates that a beat phenomenom is present. Consequently, the damping values shown should not be used in prediction, but the damping values of the separate modes should be extracted from the signature by a method such as described in reference 8. Note that methods such as reference 7 for autocorrelation do not apply to randomdec signatures.

From the above examples, we see that when signatures of unknown systems are taken and spectral density is not calculated, the randomdec signature should be obtained for at least four periods of oscillation so that the consistency and, hence, validity of ζ_{est} can be determined.

EXPERIMENTAL PROCEDURES

As was shown for the autocorrelation method in reference 2, there are many pitfalls of analysis which affect damping values obtained from random data. These problems have been studied for the random decrement method by analysis of computer-generated data and by experience with the randomdec on-line computer at Ames Research Center. In this section the problems are discussed and recommendations are made.

14

Calibration

Accurate measurements in any experiment require calibration of the equipment. Figure 16 shows the steps to be taken in calibrating a randomdec computer. An input test signal of a sine wave generator is needed which covers the frequency range in which measurements are to be taken. The figure is self-explanatory so only a few comments will be made. The setup on figure 16 assumes that the calibration of the transducer and preamplifier is known so that volts can be converted to physical units. Also the frequency response characteristics of the band-pass filter (i.e., fig. 17(a)) should be known so that the effect of filtering can be estimated. The amplifier should be a calibrated variable-gain amplifier so that the averager can be operated over its full dynamic range. The main setting of the randomdec which has to be made is to check the zero detectors as shown. Once the band-pass filter settings are known, it is good practice to take a signature of the filter using a calibrated random input before and after a test. This is a simple way to test the filter to make sure that it has not changed during the test. Some typical filter signatures are shown on figure 17(b).

The effects of the filter on the rms output of a single-degree-of-freedom system should be known for the type of filter being used so that amplifier settings can be estimated when filter settings are changed. This is also needed to convert y_s from volts to physical units. The effect of R-C filters on the filtered output, σ_F, is shown on figure 18 for various ratios of filter cutoff frequency to natural frequency of a single-degree-of-freedom system.

Aliasing

In reference 4 it is shown that sine waves which have frequencies above and below the Nyquist frequency (sample rate/2) may pass through the same points if they are taken at equal time intervals. Hence, when data is digitized the frequency components above the Nyquist frequency are folded back into components below the Nyquist frequency. To simulate this effect, a very lightly damped mode was programmed at a frequency which would fold back on the single-degree-of-freedom system with a damping ratio of 0.02 as shown on figure 19. It may be seen that a large error in the measured value of damping could be caused by the folding back of

the high-frequency mode. This problem is ordinarily avoided by passing the signal through a low-pass filter prior to digitizing. The figure serves as a reminder that aliasing is a fundamental problem which affects randomdec as well as autocorrelation and spectral density.

Input Distortion

In reference 2, it was shown that the autocorrelation signature is distorted by an input spectrum such as isotropic turbulence, and an expression for the distortion was given in terms of the 3 dB frequency, ω_1. Distortion measurements of randomdec signatures were made on the digital computer and are shown on figure 20. It may be seen that the randomdec distortion is about half the distortion with the autocorrelation signature. In either case, input distortion may be avoided by measuring damping as shown on figure 12.

Two-Mode Response

Another problem which may cause trouble in damping measurement is the occurrence of two modes with frequencies so close together that they cannot be separated without distortion by filtering. To study this problem, the time history of a two-degree-of-freedom system with closely spaced natural frequencies was generated, and the randomdec signature was computed as shown on figure 21. A check point of the theoretical free vibration decay curve is shown to fall on the randomdec signature.

For comparison, the autocorrelation function was calculated and it may be seen that it differs considerably from the randomdec signature. (Autocorrelation was only calculated for the range shown because of limited computing time available.) This is probably due to cross products which occur in the autocorrelation of closely coupled modes as discussed in reference 7, p. 28. In this reference, the separation of frequency and damping is accomplished by taking a one-sided Fourier transform of the autocorrelation function, and then by applying a Kennedy and Pancu analysis in the complex plane. In all, three Fourier transforms are required in the method. It appears that the randomdec method offers a much more direct and rapid means for separating closely coupled modes. The randomdec computation itself proceeds faster than a single Fourier transform; and, since the signature is undistorted by cross products, a direct curve

16

fitting method such as described in reference 8 may be used. (Note, a randomdec analysis of 4098 points required 10 seconds of IBM 360 computing time as compared to 20 seconds for a Fast Fourier transform.)

Sometimes the two-mode problem can be solved by location of the transducer on the node line of one of the closely spaced modes. If this is done, then two transducers are needed to measure the damping of the modes simultaneously. In most applications the structural modes, shapes, and frequencies are known ahead of time and the transducer location can be chosen to avoid response time histories with closely spaced modes. If mode shapes are unknown, then locations must be chosen by trial and error or by an educated guess.

Selection of Sample Rate

When a random force excites a structural mode of a given frequency, the output time history does not contain an infinite number of independent points, since adjacent points are correlated. (See Appendix A.) A sine wave time history, for example, may be described by its amplitude and phase and hence has only two independent measurements. Any curve, then, which may be described by a Fourier series may be described by a number of points equal to two times the number of terms in its Fourier series. Hence, if we are to extract all of the information from a time history, we must sample at a rate equal to two times the frequency of the highest Fourier series component. If we sample at a higher rate, the measured points cannot be independent and some sort of averaging means must be used to obtain the independent values. Oftentimes the sample rate is set equal to 4 or 5 times the highest frequency of interest, since a low-pass filter must be used to avoid aliasing and the higher sample rate is selected to put the flat portion of the filter over the frequency range of interest. As shown in Appendix A, randomdec signatures are relatively insensitive to low-pass filtering so that the sample rate requirements will depend on the degree of resolution desired in the signature. For failure detection, a sample rate of only 2 times the frequency of the failure mode is needed. For damping measurement, 16 times the frequency of the highest mode of interest is desirable to define the signature adequately. At the 16-times rate, the signature has a definition of 16 points per cycle, which for the 4-cycle signature recommended results in the modest requirement of storage of a 64-point signature.

Number of Segments

Selection of N = 500 seems to be an adequate choice of the number
of functions for an accurate signature. The effect on accuracy of more
or less functions may be estimated from Appendix A. Also, the time
required to obtain this number of functions for planning tests may be
obtained from Appendix A.

Transducer Location

A dynamic time history from a single transducer does not necessarily
contain all of the information needed to describe the system completely.
If the measurement is taken at a node line for example, information on
that mode will be missing. Thus we see that on a structure, the resolution
of the measurement needed to extract information on a particular mode is
very dependent on transducer location. If a single transducer location is
to be used, then a point must be found which has a sufficient amplitude in
all modes of interest (e.g., a wing accelerometer would most likely be
placed near the wing tip and strain gages near the root). In many cases,
the desirable location from a resolution standpoint may not be practical
for other reasons (e.g., accessibility, nearness to noise sources or elec-
trical disturbances, extreme environment such as hot spots, etc.). In
general, we have to select the modes of interest or section of the structure
which we wish to define, and we locate our transducers at points which
emphasize this information and de-emphasize extraneous information.

CONCLUSIONS

Studies of randomdec signatures obtained from data generated by a
digital computer and by experiments with structural models have led to
the following conclusions:

(1) For single and multi-degree-of-freedom linear systems, the
randomdec signature is equivalent to a free vibration decay curve with
an initial value at the selection amplitude.

(2) The randomdec signature provides a curve which is stable in
form and scale under a wide range of ambient vibration conditions and as
such has application as a failure detector and as a damping measurement
method.

18

(3) For narrow-band time histories, the randomdec signature compu-
tation is statistically more efficient for failure detection and damping
measurement than spectral density or autocorrelation, and hence is more
suitable for on-line application to these problems.

(4) Experimental examples of failure detection indicated the feasi-
bility of detecting loose joints and incipient structural failure. However,
considerably more experimental work is needed to define the optimum trans-
ducer locations and frequency range needed to detect a particular flaw to
a given sensitivity.

(5) Experimental examples of damping measurement indicated that
damping of an isolated mode could be measured and that the precision of
the damping measurement could be specified. For modes which are close in
frequency, the beat phenomenon was detected and a means for separating the
damping ratios and frequencies was indicated. Further work is needed to
define the limitations and precision of measurements for the multi-mode
case.

Nielsen Engineering & Research, Inc.
    Mountain View, California
        October 25, 1972

APPENDIX A

STATISTICAL PROPERTIES OF RANDOMDEC SIGNATURES

The randomdec process evolved as a result of experiments in stratification of autocorrelation functions of the response of nonlinear systems to random inputs. Some of this work has been published in reference 2 and some was used just to develop the concept. When it was found that randomdec gave unique signatures under a wide range of conditions, it was decided that the primary need in its application was to define its statistical properties. For this purpose a digital program in Fortran IV was written for the Ames Research Center IBM 360-67 computer. The program had the capability of generating random inputs and the response of linear systems including R-C filtering, and calculating from this time history randomdec signatures, standard deviation, autocorrelation, and spectral density. Figure 22 shows a typical narrow-band time history generated by the program and one measured on a model in a wind tunnel. The time histories generated by the computer program appeared to be realistic simulations of the time histories which were encountered in practice. The advantage of computer-generated data was that the exact properties of the system were known and could be compared with values obtained from signatures of the random output time history.

Most of the work was conducted on a linear single-degree-of-freedom system which admittedly is an idealized problem, but it does form the foundation for development of the concept. Figure 23(a) shows part of a time history which was generated for a single-degree-of-freedom system with a damping ratio of 0.02 and a period of 16 time units. Two randomdec samples are shown for illustration. The first one $G(16)$, is measured 16 time units after y crosses y_s with a positive slope. The second one, $H(16)$ is measured 16 time units after y crosses y_s with a negative slope. Figure 23(b) shows the average of all such samples over a record length of 4098 points for sample lags, Q, from 1 to 24. This is called the "randomdec signature". The point for $Q = 16$, $AVT(16)$, is used to check the signature measured damping against the exact value. For a damping ratio of 0.02, $AVT(16)/y_s$ should be 0.88. Average of plus-slope values (AVG) and minus-slope values (AVH) is also shown.

20

Before the above comparison can be made with significance, the distribution and independence of the samples must be established. Figure 24 shows the cumulative distribution of a typical set of samples of the G(16) and H(16) values plotted on normal probability paper. (See reference 9, p. 56.) The closeness to the straight line indicates that the distribution is approximately normal. The figure also shows that the mean value is approximately equal to 0.88 of y_s, which is the value expected for $\zeta = 0.02$. Also the standard deviation (σ_ϵ) of the measured values is seen to be 2.8 by the intersection of the 1σ (84 percent) value.

Since a certain amount of overlap occurs in the randomdec sampling process (i.e., when y_s is near a peak, G and H values are nearly the same), the degree of independence was checked as shown on figure 25(a) for $y_s = 0$; 25(b) for $y_s = \sigma_y$, and 25(c) for $y_s = 2\sigma_y$. Linear regression lines, $\overline{H}_G$ and $\overline{G}_H$, were calculated as shown (ref. 9, pp. 191-204). The square root of the product of the slopes gives a correlation coefficient estimate of $r = -0.38$, 0.15, and 0.71 for the three selection levels. Hence, when the selection level y_s is near the rms level of the signal, the measurements taken following a plus slope and then a minus slope on the same peak are nearly independent (small r). For low and high levels of y_s, the measurements on the same peak tend to become more dependent.

Figure 26 shows the reason for the increase in correlation at the high and low selection levels. At the $2\sigma_y$ level the plus- and minus-slope samples tend to be taken near peaks most of the time, which tends to make the time difference between G(16) and H(16) samples small; and since the physical system cannot move very far, the values tend to be correlated. At the zero level, the samples tend to be separated in time by one half a period, and because the process is narrow band, the G(16) and H(16) values tend to be of opposite sign and of similar value which results in the negative correlation of figure 25(a).

In an on-line computer, the time overlap in the sampled segments of the time history leads to some complication. If the speed of obtaining the signature is not critical, segments may be taken without overlap. For example, on figure 3, instead of taking the segments shown, one would take the plus-slope segment starting at t_1, then the minus-slope segment

Appendix A

starting at t_4 and so on. Figure 27 shows the correlations of samples taken in this way and it may be seen that the correlation estimate is quite small ($r = 0.08$).

With the distribution and dependence of samples established, a hypothesis test of randomdec was conducted using 25 independent cases of 4098 points each of random inputs with a normal distribution and a standard deviation of 1. The confidence boundary is given by

$$0.88 \pm \frac{c\sigma_\epsilon}{y_s \sqrt{(2 - r)K}} \qquad \begin{matrix} c = 2.05 & (96\% & \text{confidence}) \\ c = 2.88 & (99.6\% & \text{confidence}) \end{matrix} \qquad (A-1)$$

where σ_ϵ is the standard deviation of the randomdec process, r is the correlation estimate, and K is the number of peaks encountered at the selection level. Note that $(2 - r)K$ is an estimate of the number of independent samples and that in this case r is an average of values which range from 0 to 1 depending on whether the selection level was near or far from the peak. The linear weighting was selected as a first-order approximation. As shown on figure 28, about 8 points occurred at the 96-percent confidence level compared to 10 expected and 1 point at the 99.6-percent level compared to 1 expected. Hence, in the 250 cases calculated no significant evidence has been found to justify rejection of the hypothesis.

During the hypothesis test, it was noted that when $AVT(16)/y_s$ was above 0.88, the rms of the output (σ_y) tended to be high and vice versa. To show this effect a different symbol was used depending on whether σ_y of the case was above or below the average of the 25 cases ($\overline{\sigma}_y$). The predominance of the circles above 0.88 and squares below is apparent. This trend indicates that when the rms of the output is higher than usual, the signature will tend to give a value of damping ratio which is too small and vice versa. This effect is a result of the accidental time sequence of the amplitudes of the random inputs in finite time.

From the above it appears that the signature of a single-degree-of-freedom linear system excited by wide-band random noise is equivalent to the free vibration decay curve with an initial displacement. In practice we often encounter systems excited by band-limited noise; or in order to obtain an effective single degree of freedom, the time history has to be

22

filtered. The question is "What effect does filtering have on the signature?" In order to evaluate this, a particular case of 4098 random inputs to the single-degree-of-freedom system with a damping ratio of 0.02 was selected for the filter studies. The program was capable of filtering the time history in any combination of high- and low-pass R-C filters cascaded and with varying cutoff frequencies (ω_1 is defined as the half-power or 3 dB point frequency of the filter). Figure 29 shows a typical distortion effect of a low-pass filter. Distortion is judged by the change from the unfiltered signature at the 1/2, 1, and 1-1/2 period points (Q = 8, 16, 24, respectively).

Figure 30(a) shows the effect of a low-pass, single-pole filter and it may be seen that little or no distortion occurs for filter frequencies as low as two times the natural frequency of the system. A similar effect on the signature would occur if instead of filtering the output, the input to the system were isotropic turbulence with a half-power point at ω_1. In judging the distortion, it should be noted that a very sensitive scale has been used on the figure and that even at $\omega_1/\omega_n = 1$, the distortion is actually only 1 percent of the selected level (y_s).

Similar results are shown in figure 30(b) for a cascaded low-pass filter which gives somewhat greater distortion. However, it must be remembered that these are the basic distortions of the filter on the system and that in actual practice the off-resonant effects of other modes can also distort the signature. The distortion caused by the filter must be weighed against the distortions of extraneous modes which it eliminates. This is beyond the scope of the present report and is only mentioned here to put the results in the proper perspective.

Figure 30(c) shows the results which were obtained with a high-pass, double-pole filter. Some distortion is evident at Q = 16, but this is small, being only a little greater than 1 percent of the selection level. The basic distortions of the high-and low-pass filters (fig. 30) serve as a guide to filter selections in specific applications. It appears that distortion is not a serious problem except in the extreme cases $\omega_1/\omega_n = 0.5$ for the low-pass, single-pole filter and $\omega_1/\omega_n = 1$ for the low-pass, double-pole filter.

Appendix A

The objective of this study was to develop expressions for record length needed to obtain signatures of a given precision relative to the selection level. The latter part of this statement has been underlined to emphasize the difference between the approach used here, and the usual approach in spectral density and autocorrelation. The expressions in reference 4 give the standard deviation of the individual points on the signature rather than the standard deviation of the individual points relative to a reference level as given here. This distinction is very important in precision measurements of damping ratio and is particularly critical to the uniqueness of the signature of a system with nonlinear damping under variable input conditions.

Solution of the record length problem requires knowledge of the effects of filtering and damping ratio on the standard deviation of the signature. Figure 31 shows these for the filters discussed in the previous section and for the unfiltered case with various damping ratios. As may be seen, the standard deviation is insensitive to these variables to a ±10-percent level with the exception of the extreme filter settings which may be excluded because of their high distortion. These characteristics of randomdec greatly simplify the solution to the record length problem.

Another variable which has to be considered is the selection level, y_s. Figure 28 shows the effect of this variable. The ordinate is $AVT(16)/y_s$ so the dispersion seen is in fractions of the selection level. For low selection levels, the scatter increases because the standard deviation, although nearly constant, becomes a larger fraction as selection level becomes lower. As selection level increases, the fractional error decreases, but the number of peaks encountered becomes fewer until finally the dispersion increases again. The fractional accuracy of the signature F_s may be expressed as

$$F_s = \frac{C\sigma_\epsilon}{y_s \sqrt{(2-r)K}} \tag{A-2}$$

where C is the level of confidence factor, σ_ϵ is the standard deviation of the signature point $(Q = 16)$, y_s is the selection level, r is the correlation coefficient, and K is the number of peaks encountered.

24

Figure 32 shows a relation for the number of peaks expected in a given time for filtered and unfiltered cases. It may be seen that the measured number of peaks from the computer runs agrees reasonably well with a predicted curve based on a Rayleigh distribution of peak values. The number of peaks encountered is:

$$K = f_n T e^{-\frac{Y_s^2}{2\sigma_Y^2}} \qquad \text{(A-3)}$$

Substituting (A-3) in (A-2) gives:

$$F_s = \frac{C\sigma_\varepsilon e^{\left(\frac{Y_s}{2\sigma_Y}\right)^2}}{Y_s \sqrt{(2 - r)f_n T}} \qquad \text{(A-4)}$$

From figure 31 we see that allowing deviations of ±10 percent that

$$\frac{\sigma_\varepsilon}{\sigma_Y|_{\zeta = 0.02}} = 0.47$$

Since on figure 31(b) it is seen that σ_ε is only weakly dependent on ζ, we may write

$$F_s = \frac{0.47 C \left(\frac{\sigma_Y|_{\zeta=0.02}}{\sigma_Y}\right) \sigma_Y e^{\left(\frac{Y_s}{2\sigma_Y}\right)^2}}{Y_s \sqrt{(2 - r)f_n T}} \qquad \text{(A-5)}$$

and using the relations for σ_Y from reference 2,

$$\frac{\sigma_Y|_{\zeta=0.02}}{\sigma_Y} = \sqrt{\frac{\zeta}{0.02}}$$

Appendix A

and substituting in (A-5)

$$F_s = 2.35 \, C\left[f\left(\frac{y_s}{\sigma_y}\right)\right]\sqrt{\frac{2\zeta}{f_n T}} \qquad (A-6)$$

in which

$$f\left(\frac{y_s}{\sigma_y}\right) = \frac{e^{\left(\frac{y_s}{2\sigma_y}\right)^2}}{\left(\frac{y_s}{\sigma_y}\right)\sqrt{2 - r}} = L$$

This factor which is a function of y_s/σ_y only varies by 25 percent for y_s/σ_y values from 0.7 to 2. This means that, for a fixed y_s, the random input, σ_r, could vary by a factor of 3 without having much effect on the accuracy at constant record length. Note that r was also a function of y_s/σ_y as was shown on figure 25.

Solving for record length, we have:

$$T = \frac{10\zeta L}{f_n}\left[\frac{C}{F_s}\right]^2 \qquad (A-7)$$

in which L is the function of y_s/σ_y given below:

y_s/σ_y	.2	.4	.6	.8	1.0	1.2	1.4	1.6	1.8	2.0
L	20	4.9	2.4	1.5	1.1	1.0	1.0	1.2	1.4	1.8

$$C = 2.06 \qquad \text{(96\% confidence level)}$$
$$1.96 \qquad \text{(95\% confidence level)}$$
$$1 \qquad \text{(68\% confidence level)}$$

When measuring damping ratio, the reference length for fractional accuracy is $2\pi\zeta y_s$ rather than y_s. Record length then becomes:

$$T = \frac{L}{4\zeta f_n}\left[\frac{C}{F_\zeta}\right]^2 \qquad (A-8)$$

26

in which

$$F_\zeta = \text{fractional accuracy in damping ratio}$$

NOTE: If no overlap is used, above equations should be multiplied by 2.

In using this equation for planning damping measurements, we must select the lowest damping ratio (ζ) which we wish to measure, the confidence level, and the accuracy desired. To minimize testing time, a selection level of 1.2 to 1.4 should be used so that L will be at its minimum value of 1. If the system has nonlinear damping, L must be selected to cover the range of amplitudes desired. In tests which are extremely costly or dangerous, the damping ratio should be monitored on-line and record length determined on-line from the equation. Such a procedure could result in a considerable cost saving and reduction in risk in wind-tunnel and flight flutter-buffet tests.

The above equations give the basic time needed to obtain signatures of specified accuracy for a single-degree-of-freedom system excited by band-limited Gaussian noise. In practice, additional variance may be introduced by added noise and inaccuracies in starting times at the selection level. Also, when more than one degree of freedom is present, the signatures contain contributions from all of the modes. This does not cause serious problems in failure detection, but it may require further processing of signatures when damping of individual modes is needed.

It is interesting to compare the above result with the equation for autocorrelation derived from reference 4, page 195

$$T = \frac{R^2(0) + R^2(\tau^2)}{4\pi\varepsilon^2\zeta f_n} \tag{A-9}$$

As ζ approaches zero, we note that the time required for a randomdec signature, equation (A-7), approaches zero as compared to time required for autocorrelation, equation (A-9), which approaches infinity. The reason for this difference is that randomdec has a fixed amplitude reference so that as ζ approaches zero and the time history becomes essentially a sine wave in a finite record, only a very short record is needed to define the signature. The autocorrelation on the other hand

Appendix A

has a variable amplitude reference which increases with the inverse of
the damping ratio and thus an infinite record is needed to define the
signature.

Using equation (A-7), we may obtain a rule-of-thumb number of segments
needed for 5-percent accuracy at 95-percent confidence level, y_s set at
σ_y and $\zeta < 0.025$.

$$Tf_n = (10)(0.025)(1.1)\left[\frac{1.96}{0.05}\right]^2 = 422$$

Using equation (A-3) for the number of peaks and noting that there are two
segments per peak, we obtain

$$N = 2K = \frac{(2)(422)}{1.65} \approx 500$$

which is the number of segments which was found experimentally to give
signatures with small variance in reference 6.

APPENDIX B

COMPARISON OF RANDOMDEC AND AUTOCORRELATION SIGNATURES

In Appendix A it has been shown that to a 99.6-percent confidence level that the randomdec signature has the same form as the free vibration curve of a linear single-degree-of-freedom system with an initial displacement. Reference 2 shows that the autocorrelation function gives this form too in the limit as record length approaches infinity. It appears, then that randomdec and autocorrelation signatures are identical in form but not in scale for linear single-degree-of-freedom systems excited by white noise. The question is "Are autocorrelation and randomdec signatures the same or are there significant differences?"

Figure 33 shows a comparison of values at the 1P point for auto-correlation and randomdec signatures of a single-degree-of-freedom system. The circled symbols represent the white noise input, and it may be seen that although agreement is fairly good that there are significant differences between signatures when record length is finite. Also shown on this figure are the effects of change in damping ratio and the filters used in figure 30. Again general agreement is good, but referring back to figure 20, it may be seen that distortion due to filtering is generally less for randomdec than for autocorrelation signatures. This might be significant in some applications, but generally speaking, there does not seem to be a significant difference between the two for the linear single-degree-of-freedom case.

Computationwise there is a very significant difference between the two signatures. For a record length of 4098 points, the randomdec calculation required 315 operations per point as compared to 16,321 for direct autocorrelation. The computational advantage of randomdec is not so great if autocorrelation is calculated by the Fast Fourier Transform. In this case, randomdec is about four times faster.

The computational advantage of randomdec becomes more and more significant as damping ratio decreases as shown on figure 33. This is a plot of the standard deviation of the 1P point on the signature with a fixed set of 4098 random inputs. As damping ratio varies, it may be seen that the standard deviation of the randomdec remains approximately constant while the standard deviation of the autocorrelation signature approaches very large values.

29

Appendix B

Perhaps the most significant difference between the two signatures
is shown on figure 21, which shows a dramatic difference for the two-
degree-of-freedom case. This result definitely establishes randomdec
as a distinctly different signature from autocorrelation. From unpub-
lished work with nonlinear systems, it is known that significant
differences occur for systems with nonlinear damping, but this is beyond
the scope of the present work.

30

REFERENCES

1. Eggwertz, Sigge and Lindsjö, Göran: Study of Inspection Intervals for Fail-Safe Structures. The Aeronautical Research Institute of Sweden, FFA Report 120, 1970.

2. Cole, Henry A., Jr.: On-the-line Analysis of Random Vibrations. AIAA Paper No. 68-288, presented at the AIAA/ASME Ninth Structures, Structural Dynamics and Materials Conference, Palm Springs, California, 1968.

3. Lee, Y. W.: Statistical Theory of Communication. John Wiley and Sons, Inc., 1963.

4. Bendat, J. S. and Piersol, A. G.: Measurement and Analysis of Random Data. John Wiley and Sons, Inc., 1966.

5. Cole, Henry A., Jr.: Method and Apparatus for Measuring the Damping Characteristics of a Structure. United States Patent No. 3,620,069, Nov. 16, 1971.

6. Cole, Henry A., Jr.: Failure Detection of a Space Shuttle Wing Flutter Model by Random Decrement. NASA TM X-62,041, May 1971.

7. Bhat, Waman V. and Wilby, John F.: An Evaluation of Random Analysis Methods for the Determination of Panel Damping. NASA CR-114423, Feb. 1972.

8. Wilcox, Philip R. and Crawford, William L.: A Least Squares Method for Reduction of Free Oscillation Data. NASA TN D-4503, 1968.

9. Dixon, Wilfrid J. and Massey, Frank J., Jr.: Introduction to Statistical Analysis. McGraw-Hill Book Company, Inc., 1957.
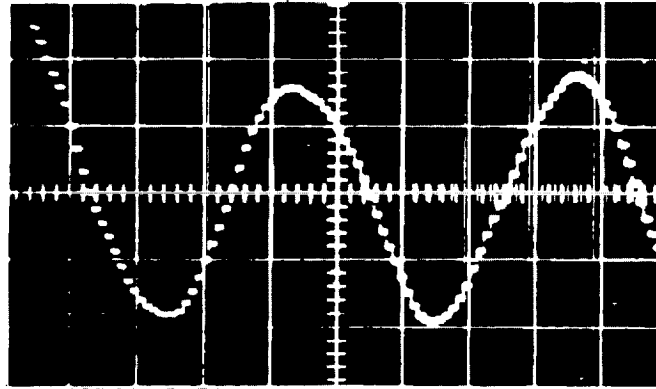
Before local structural failure
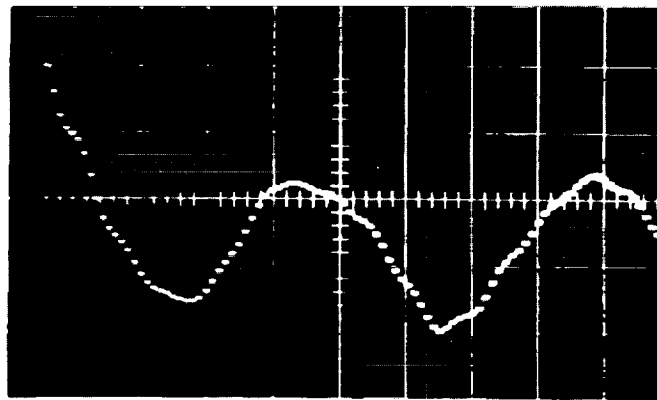
After local structural failure

Figure 1.- Autocorrelation signature of strain
gage output observed on an Apollo wind
tunnel model during test.

32

Given: Random Response (Input Unknown)
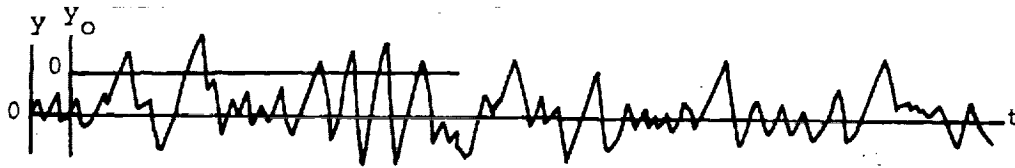
Dynamic Signatures:

Spectral Density

$$G(f) = \frac{1}{N} \sum_{n=1}^{N} \frac{2}{T} \left| \int_0^T y(t) e^{-i2\pi ft} dt \right|^2$$
$$\lim N \to \infty$$
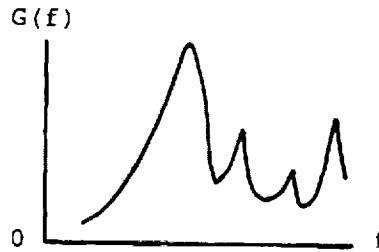
Autocorrelation

$$R(\tau) = \lim_{T \to \infty} \frac{1}{T} \int_0^T y(t) y(t+\tau) dt$$
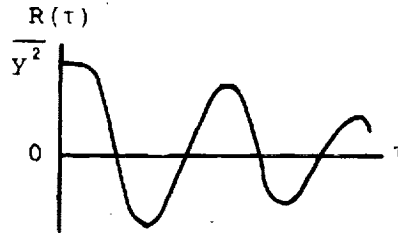
Random Decrement

$$y_o = \bar{y} - y_s$$

$$\delta(\tau) = \frac{1}{N} \sum_{n=1}^{N} y_o(t_n + \tau)$$

with conditions

$$t_n = t \quad \text{when} \quad y_o = 0$$
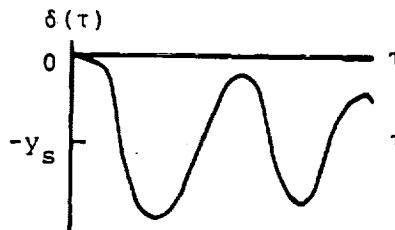
Figure 2.- Typical characteristic structural signatures
obtained from a random response.

33
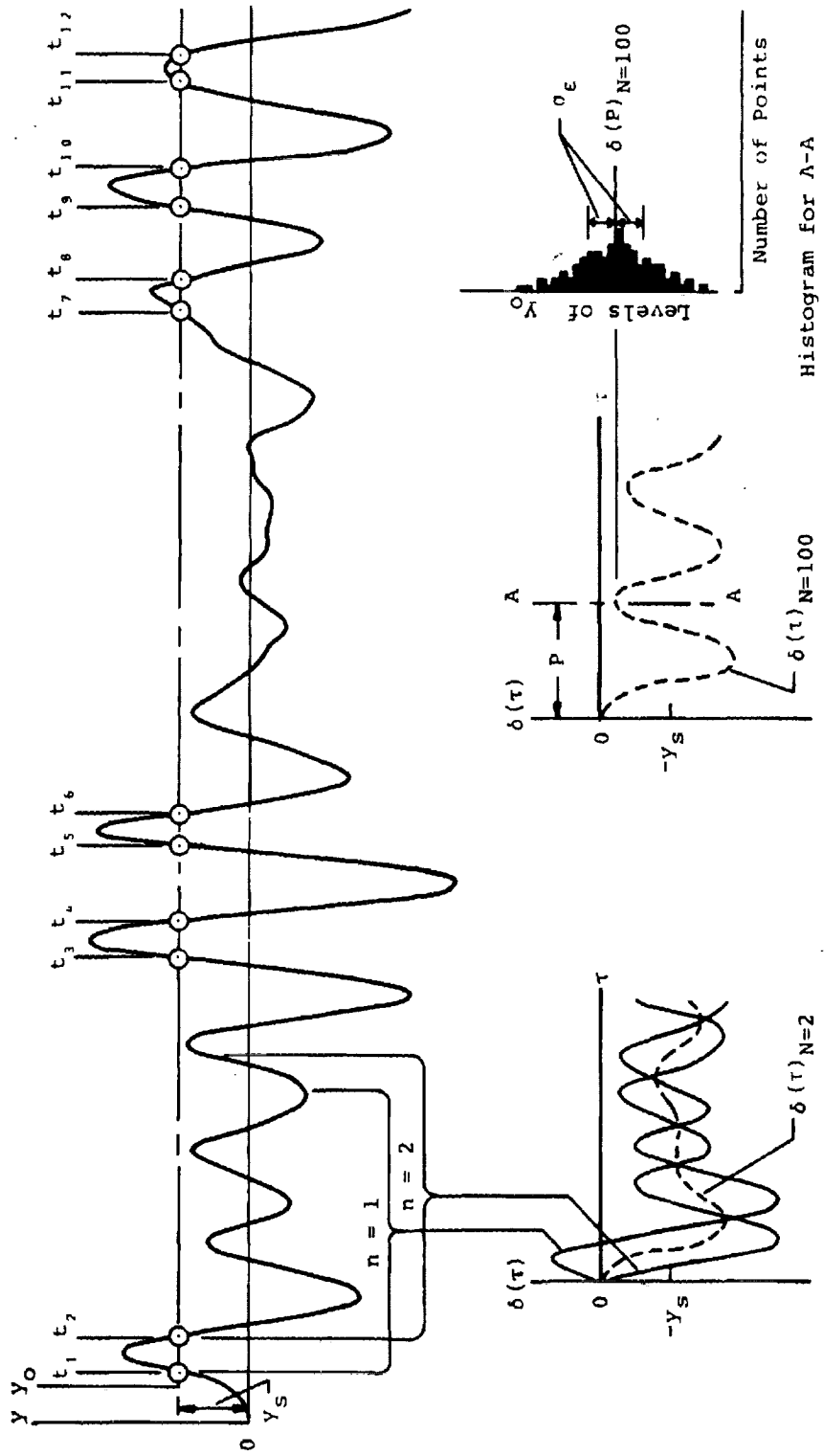
(a) Distribution of amplitude samples.

Figure 3.- Evolution of a random decrement signature.

34
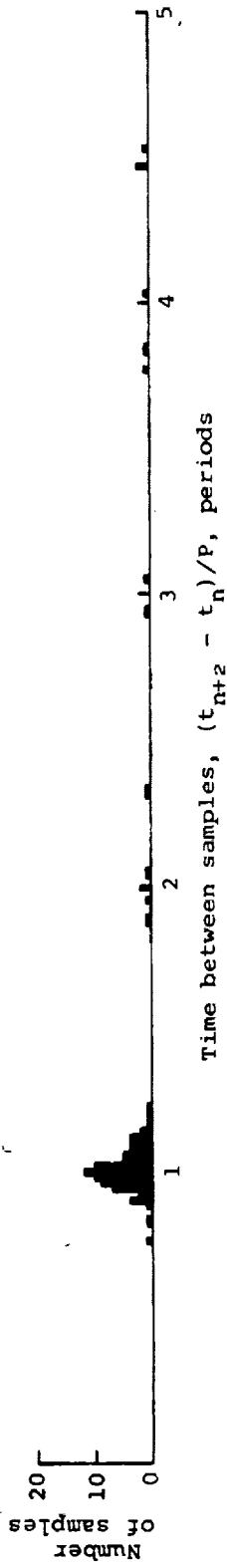
(b) Histogram of time between selected samples; $Y_s = \sigma_y$, N = 100.

Figure 3.- Concluded.

35
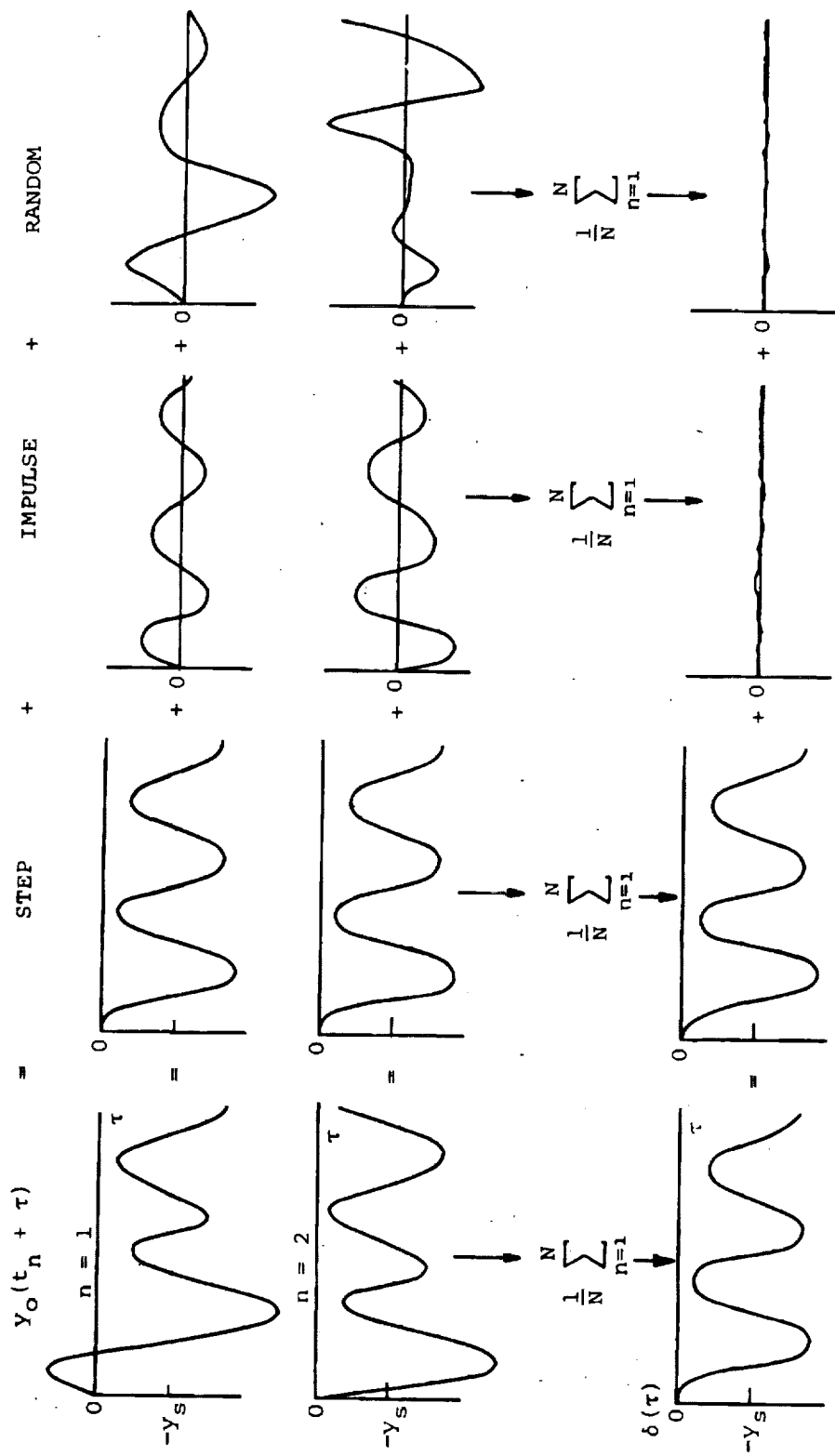
Figure 4.- Hypothesis on andomdec signature for linear systems.

36
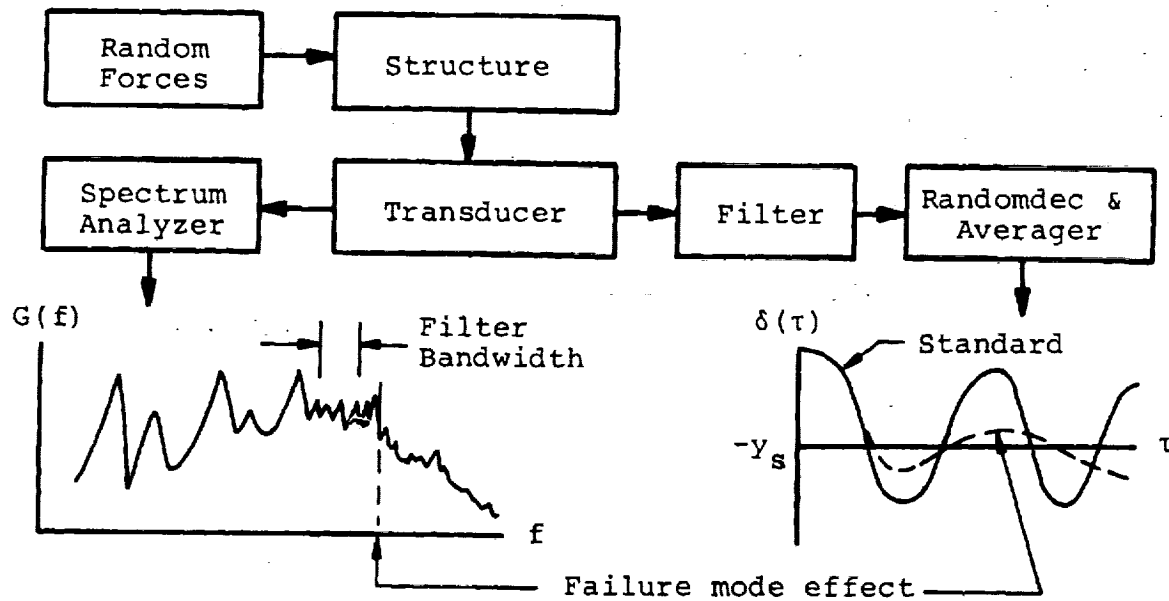
Hypothesis:

   (1) Flaw introduces additional degree of freedom.

   (2) Frequency of flaw mode decreases as flaw size grows.

   (3) Flaw mode causes change in signature by:

      (a) Dynamic coupling with modes in filter
         bandwidth.

      (b) Nonlinear coupling at subharmonic frequencies.

      (c) Friction damping.

Figure 5.- Hypothesis on the sensitivity of
random decrement signatures to flaws.

37
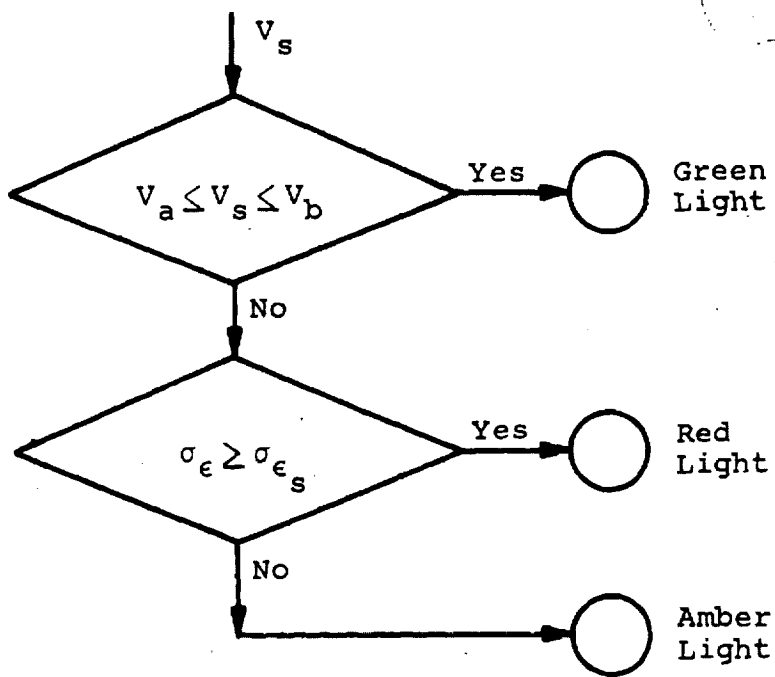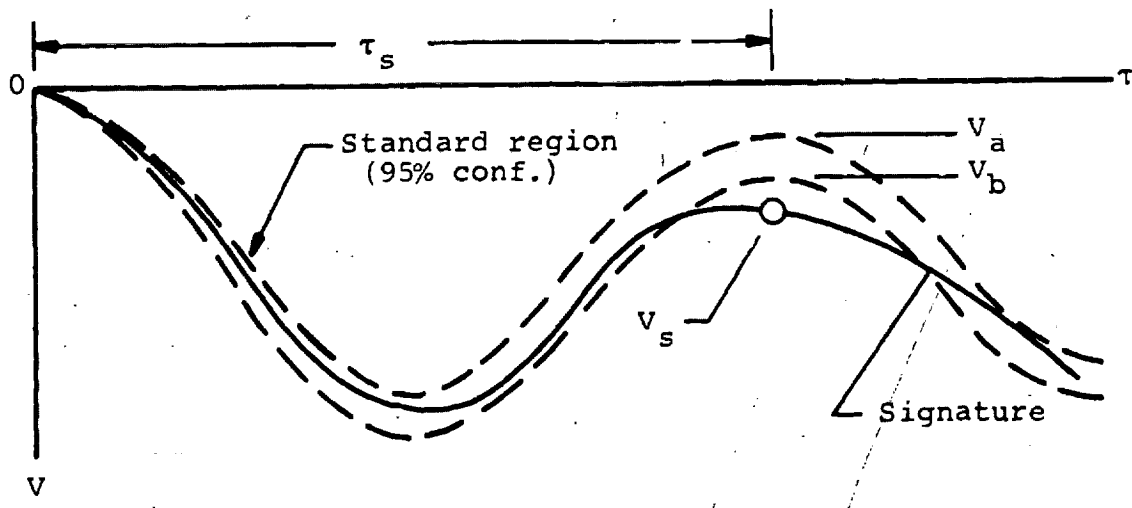
Figure 6.– On-line failure detection at a
single point on the signature.
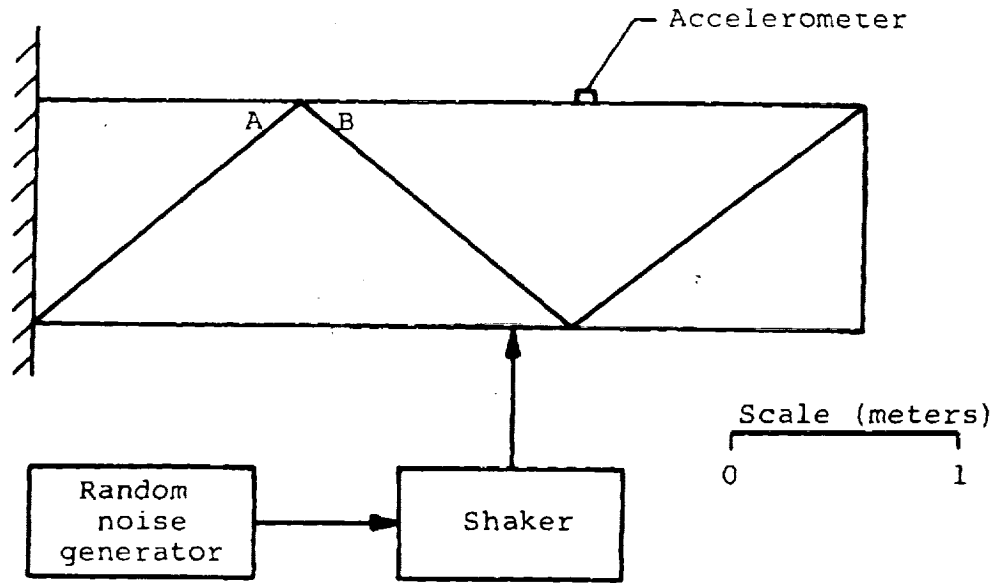
(a) Schematic experimental setup.
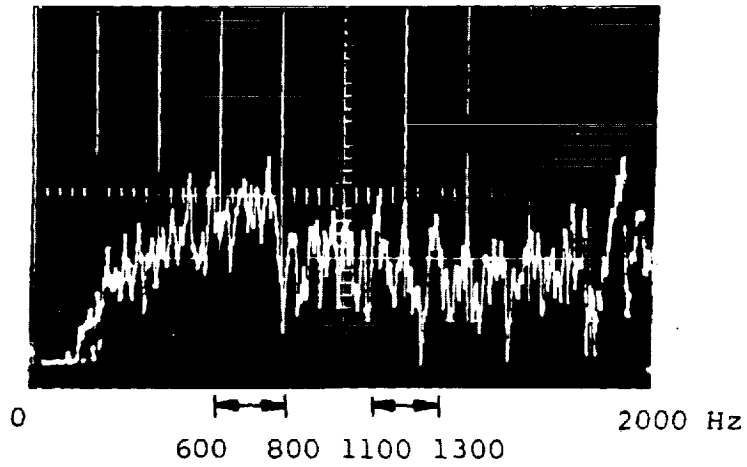
(b) Spectral density of accelerometer output.

Figure 7.- Experiment with truss
(angle steel with bolted joints).

39
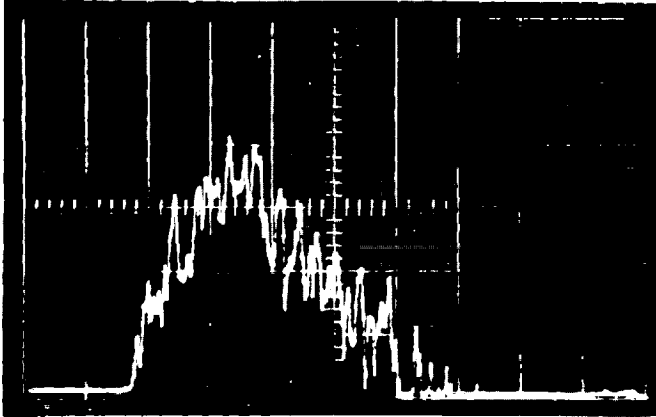
Bolts tight
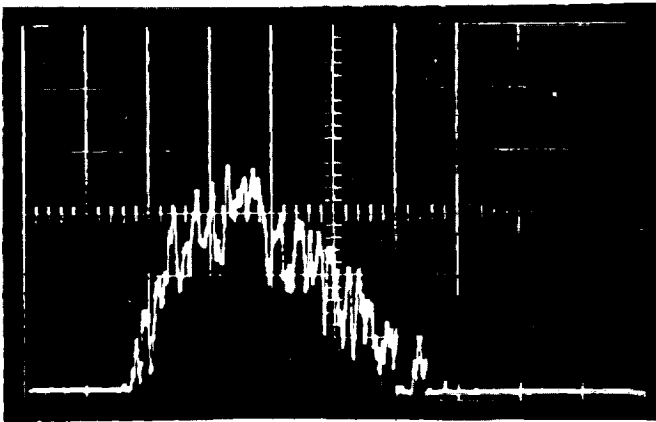
Bolts loose

(c) Spectral density with band pass
filter 600-800 Hz.

Figure 7.- Continued.

40
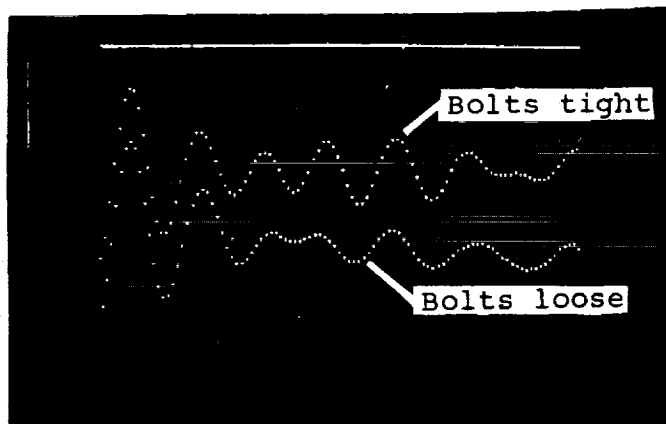
(d) Randomdec with band pass
      filter 600-800 Hz.
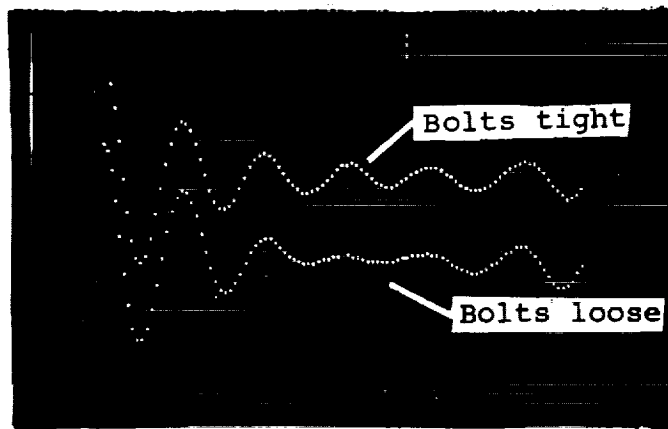
(e) Randomdec with band pass
      filter 1100-1300 Hz.

Figure 7.- Concluded.

X Strain gage

Sample
Times

0-2:45

2:45-3:00

3:00-3:09

3:09-3:15

3:15-3:22

3:22-3:30

3:30-3:40

3:40-3:50

3:50-End

Standard

Signature change

Incomplete
(Wing failed)
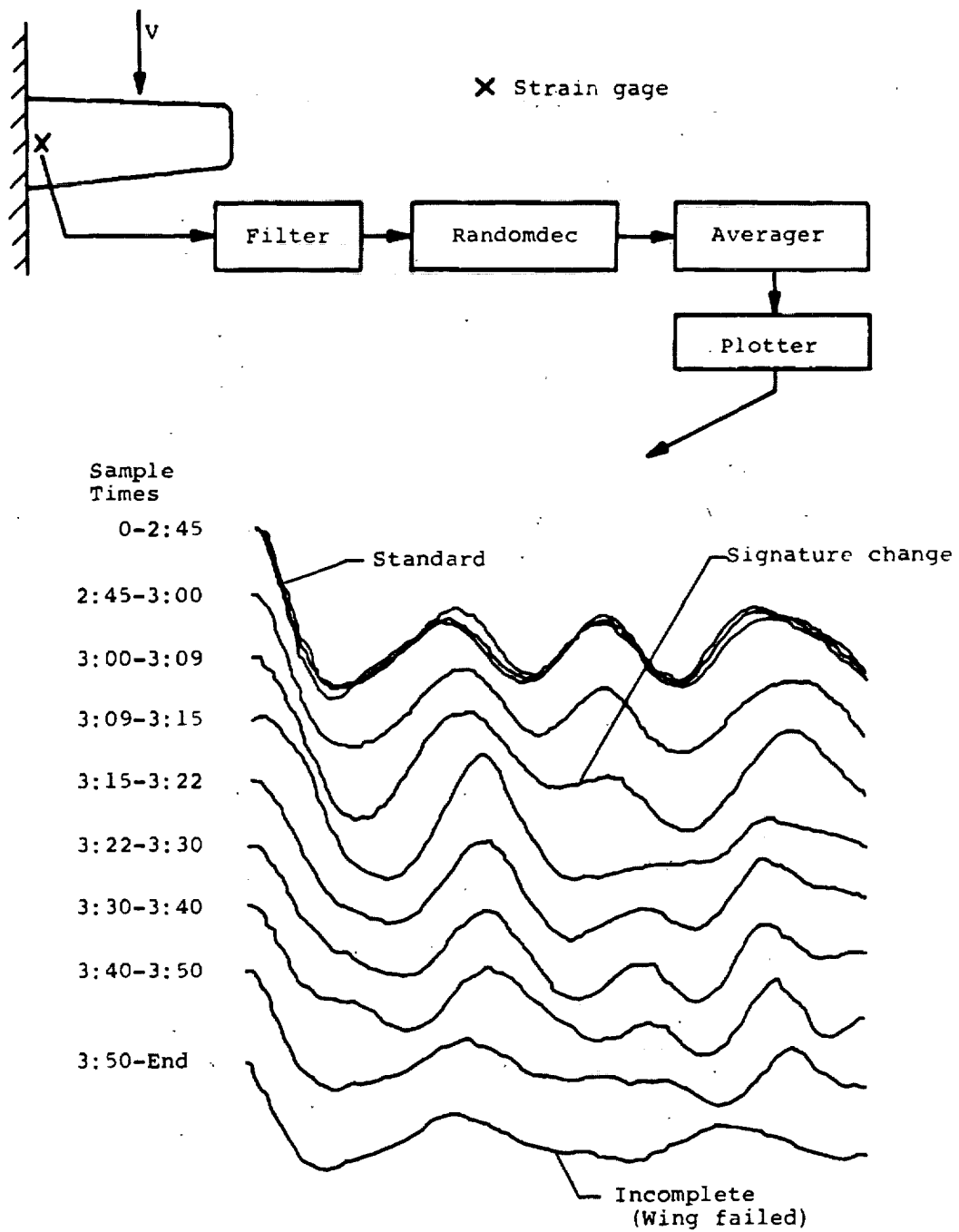
(a) Filter band-pass 200-1500 Hz.

Figure 8.- Evolution of the random decrement signature
of a wing model approaching complete failure.

42

Sample
Times

2:30-2:45

2:45-3:00

3:00-3:09

3:09-3:15

3:15-3:22

3:22-3:30

3:30-3:40

3:40-3:50

3:50-End

Incomplete
(Signal stopped)
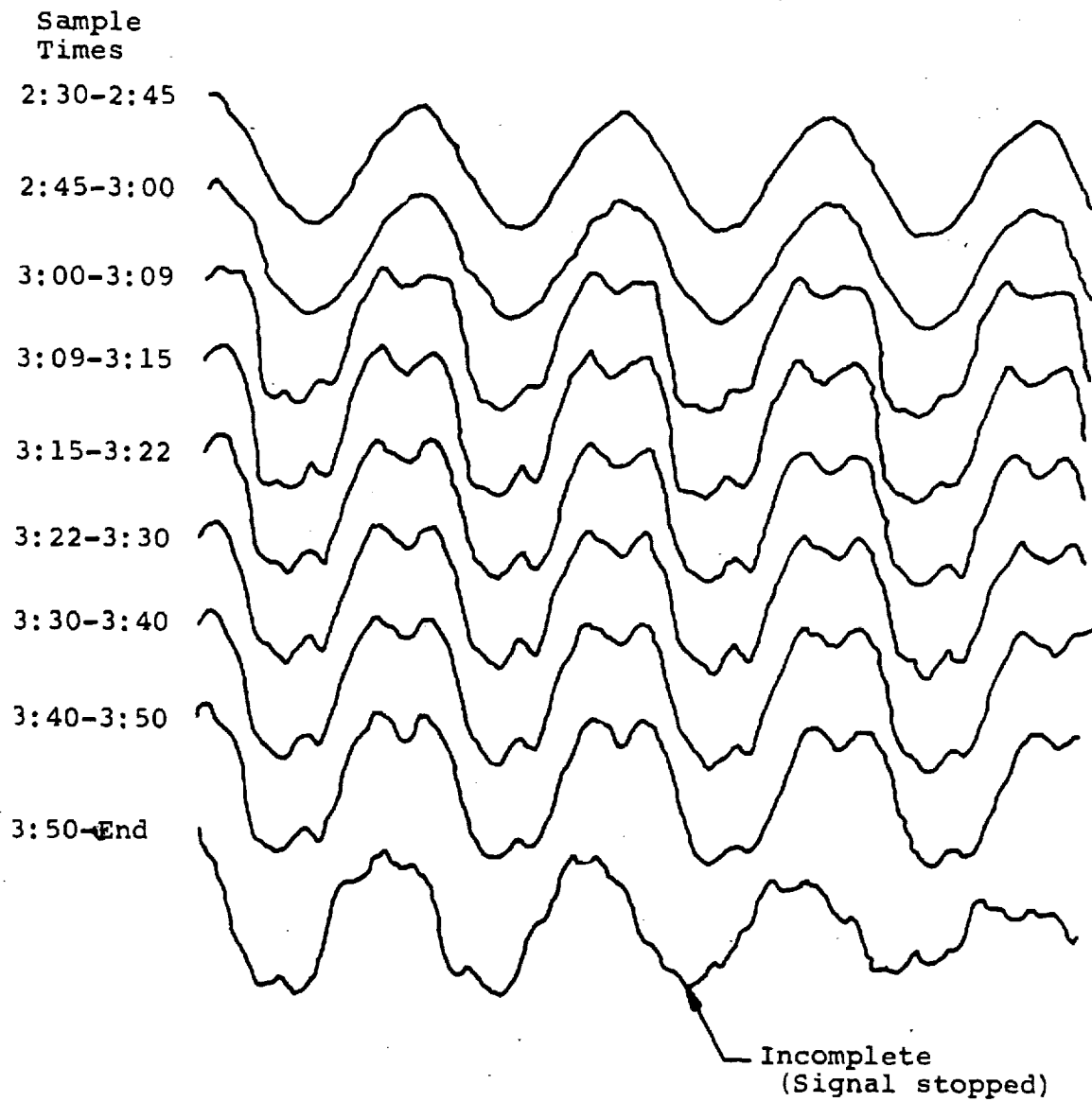
(b) No filter.

Figure 8.- Concluded.

43

TIME
min:sec ————▶ t

2:30

3:00

3:09

3:22

3:40

3:50
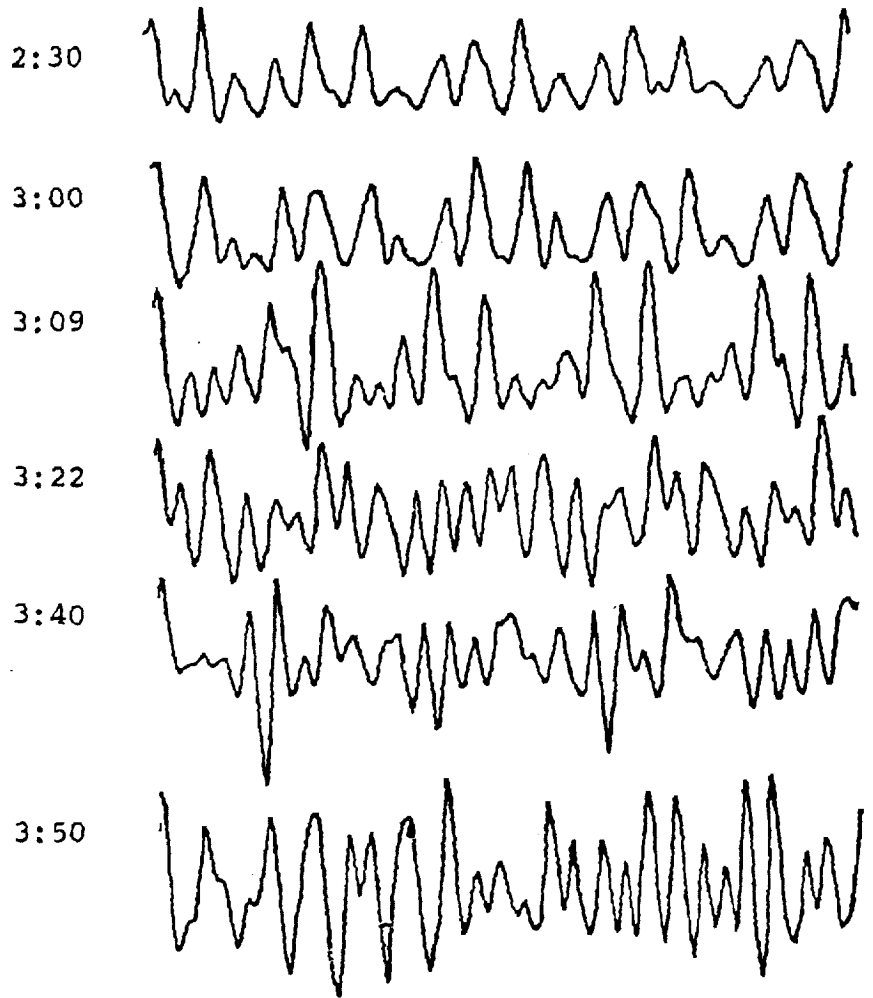
Figure 9.- Samples of time history of strain gage
output at times when signatures of figure 8
were taken (filter band-pass 200-1500 Hz).

44
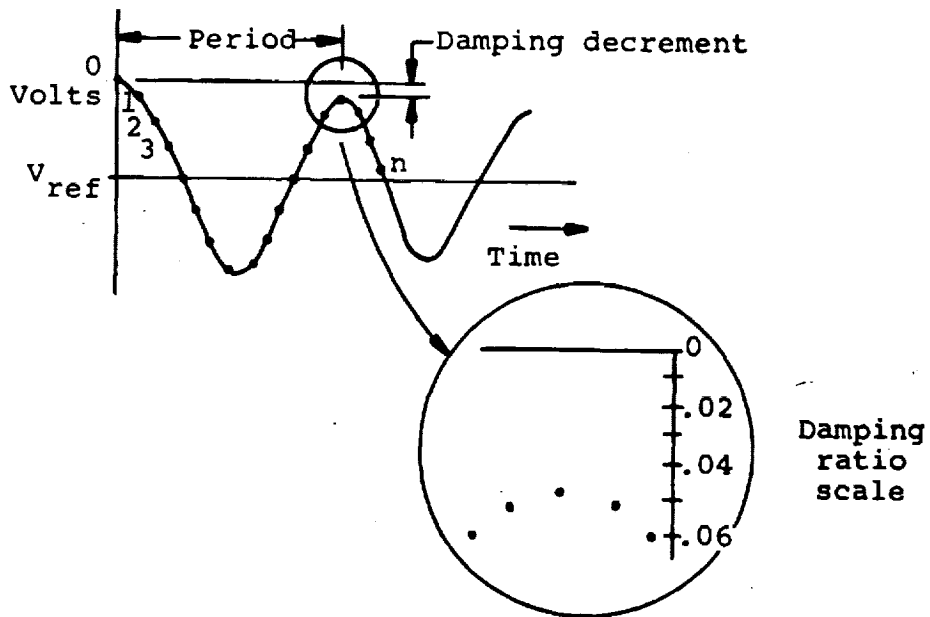
(a) Damping ratio scale on scope.
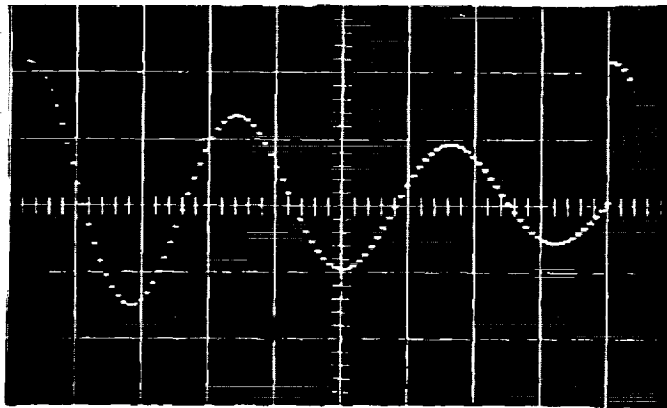
(b) Scope sweep set faster
than signature sweep.

Figure 10.- On-line damping measurement
display (no distortion).
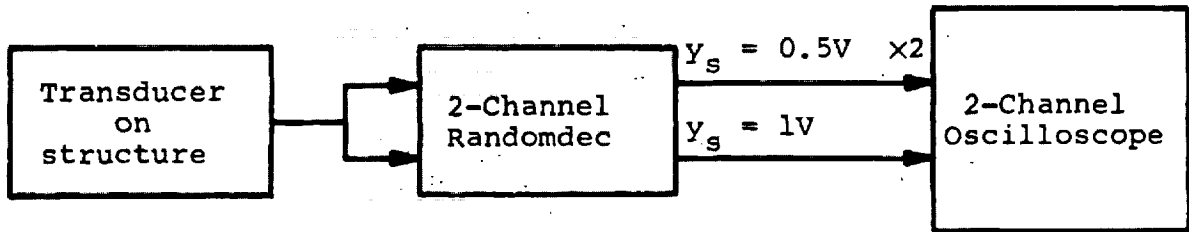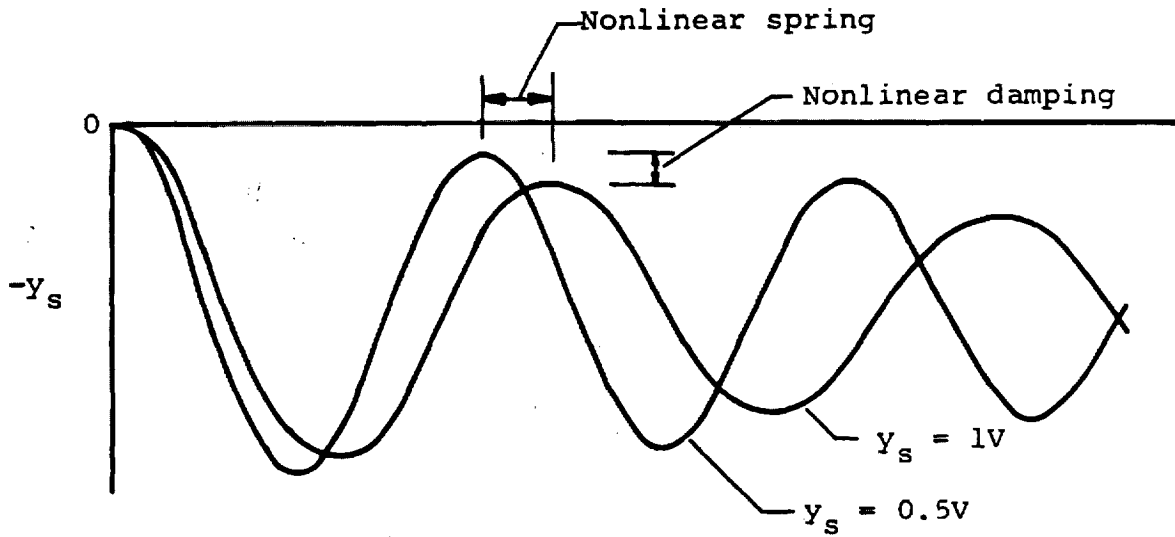
Figure 11.- On-line detection of nonlinear
effects with amplitude.
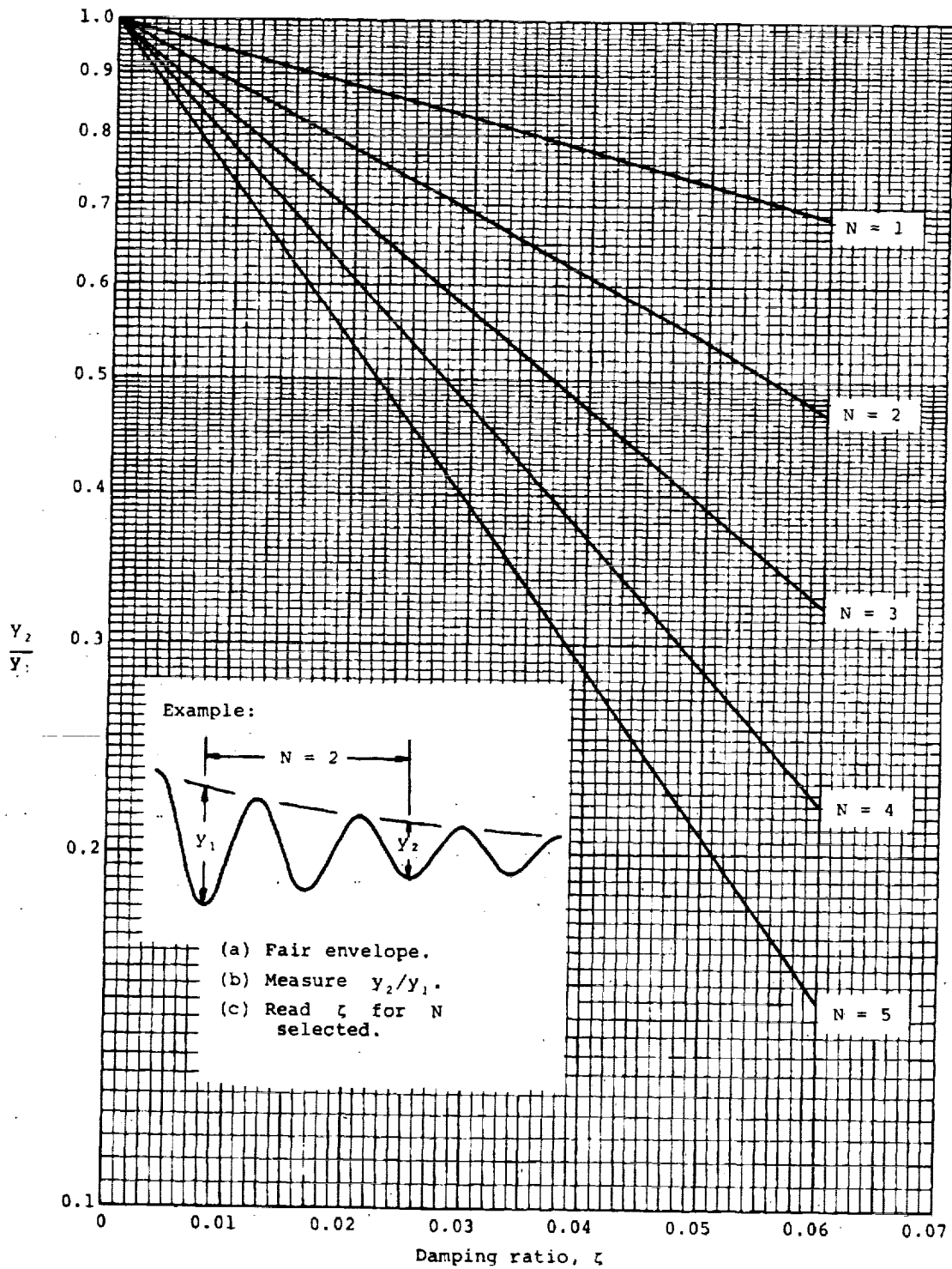
Figure 12.- Measurement of damping ratio from signature of a single-degree-of-freedom system.
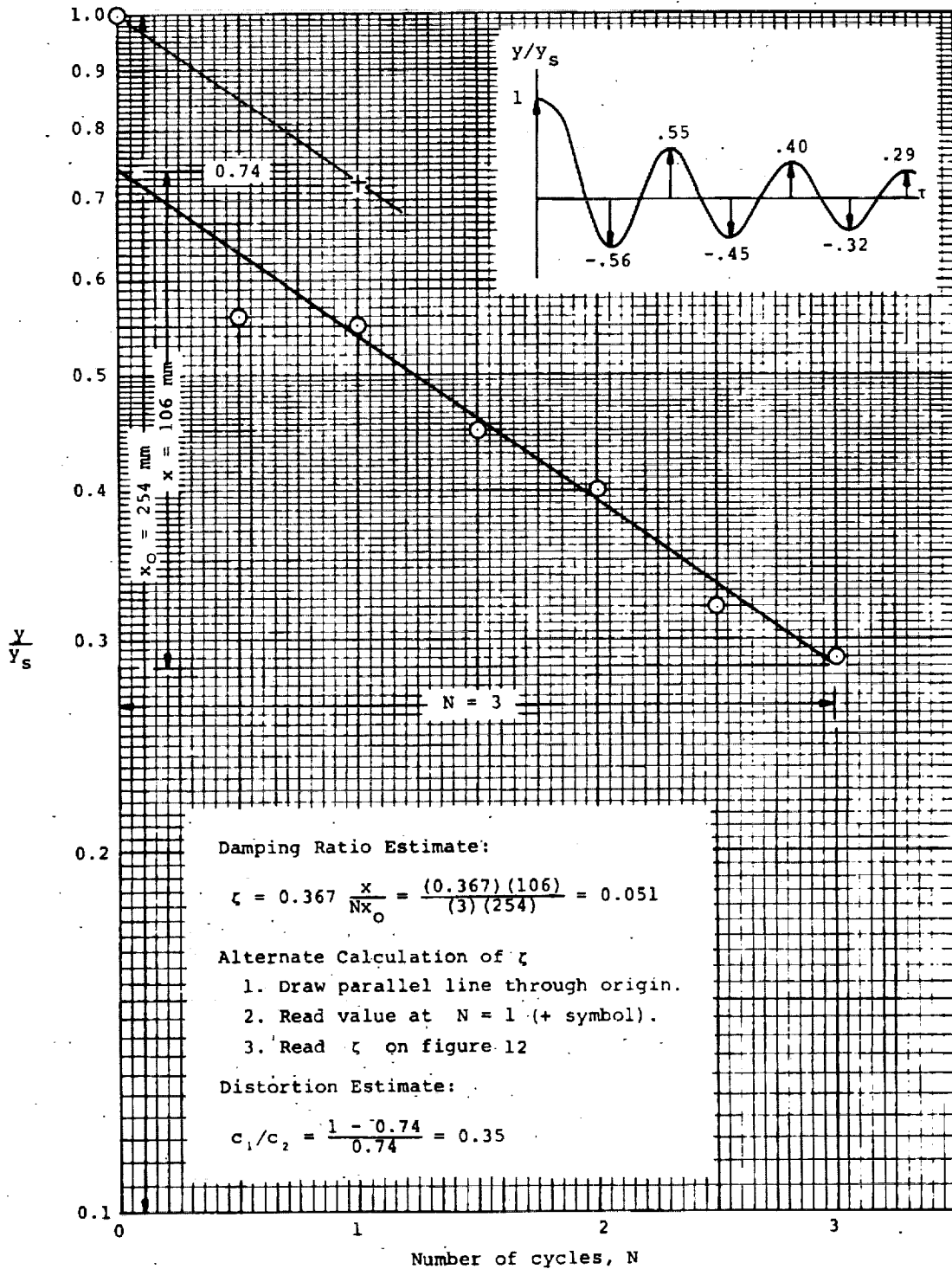
Figure 13.- Alternate method for estimation of
damping ratio including distortion estimate.
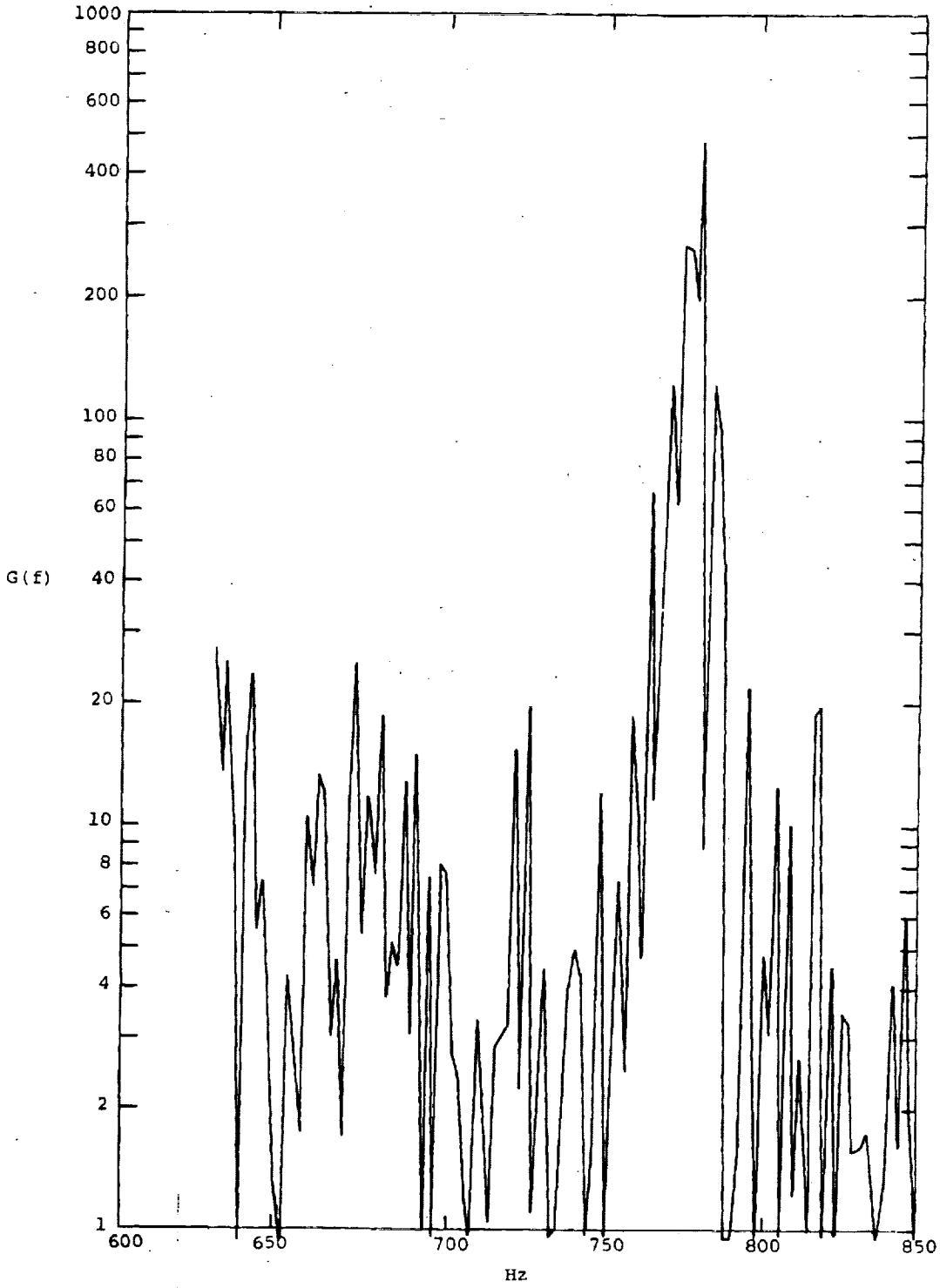
(a) Spectral density.

Figure 14.- Example of damping measurement
of an isolated mode.
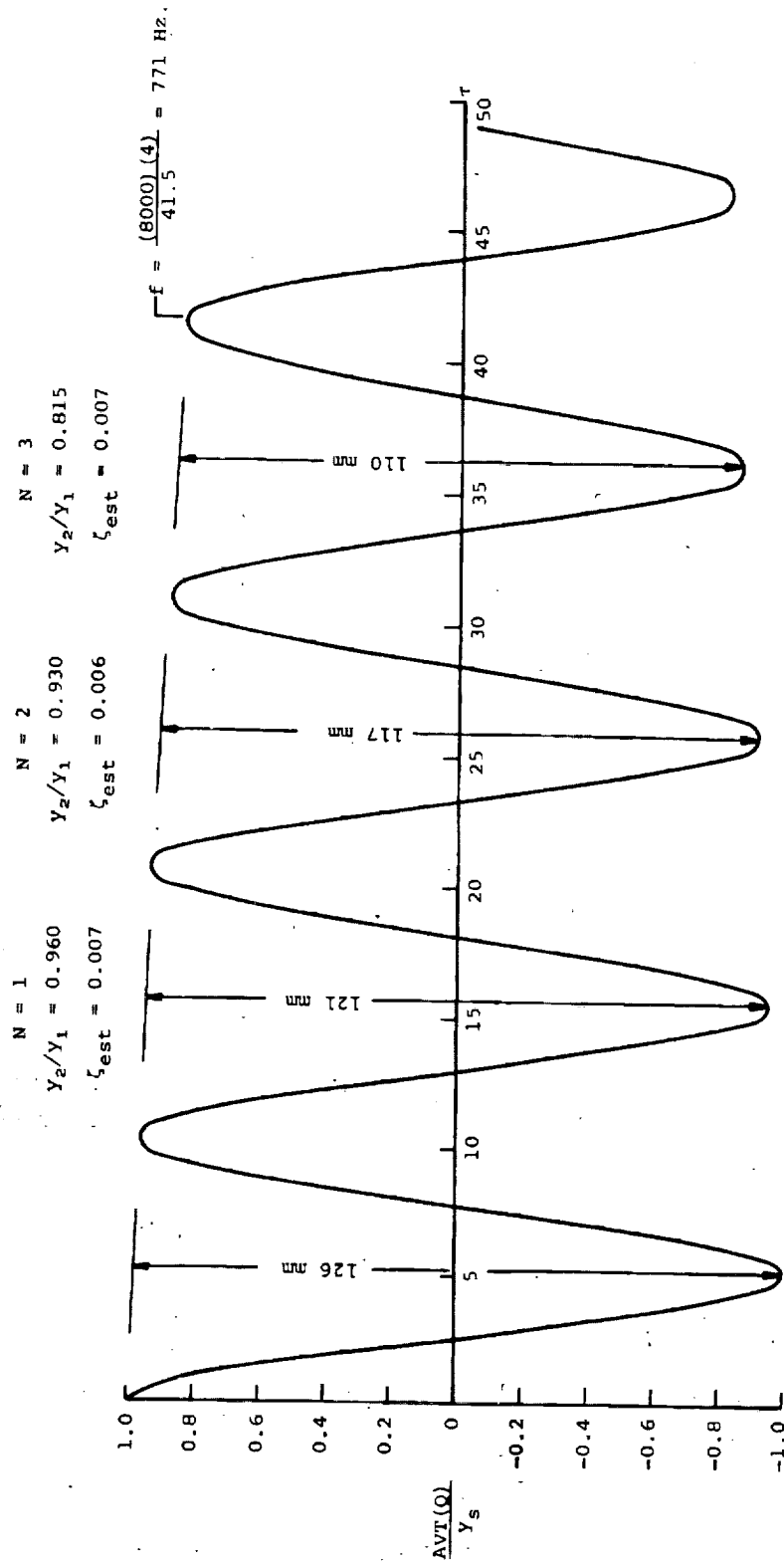
(b) Randomdec signature.

Figure 14.- Concluded.
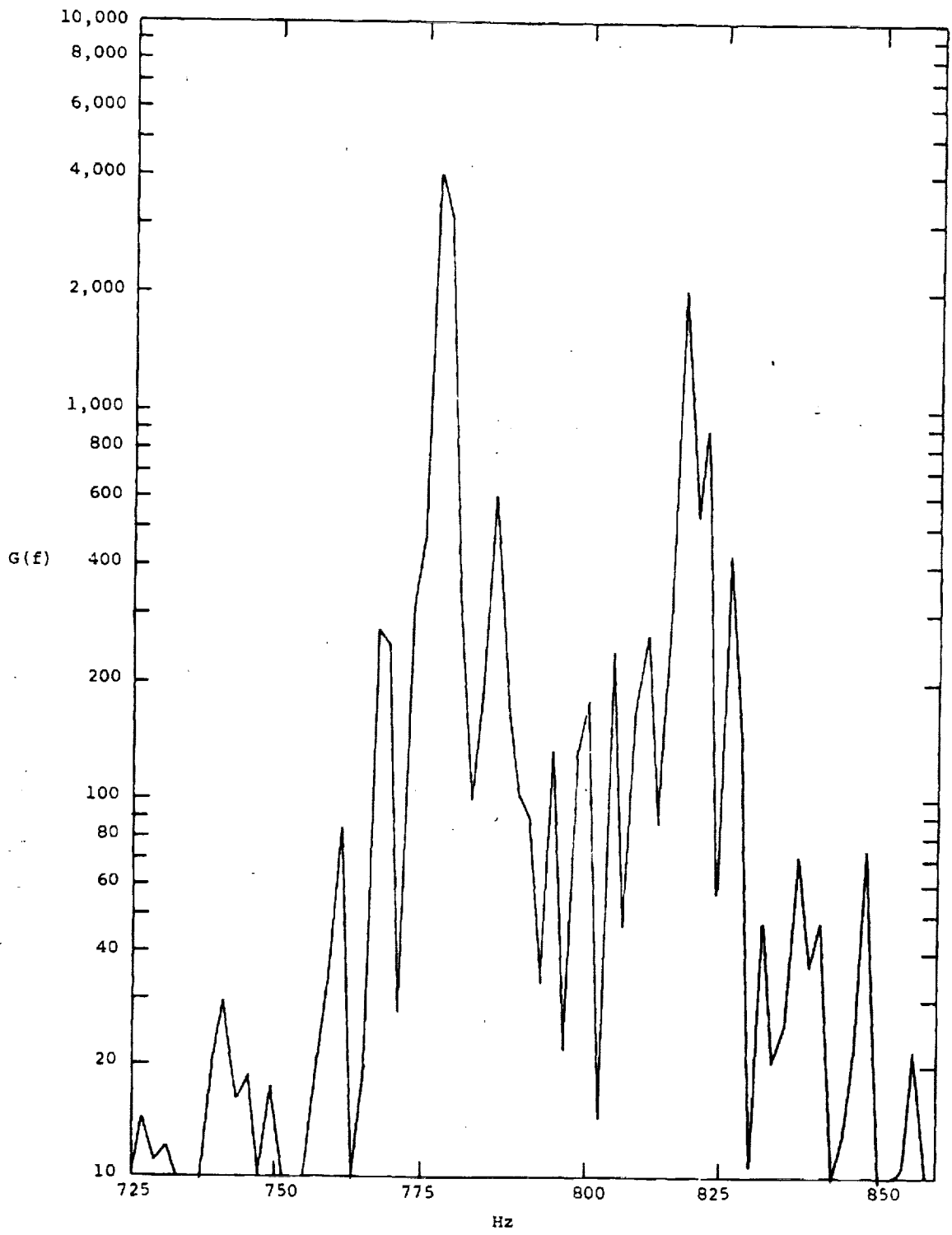
(a) Spectral density.

Figure 15.- Example of damping measurement of two modes
with nearly the same natural frequency.
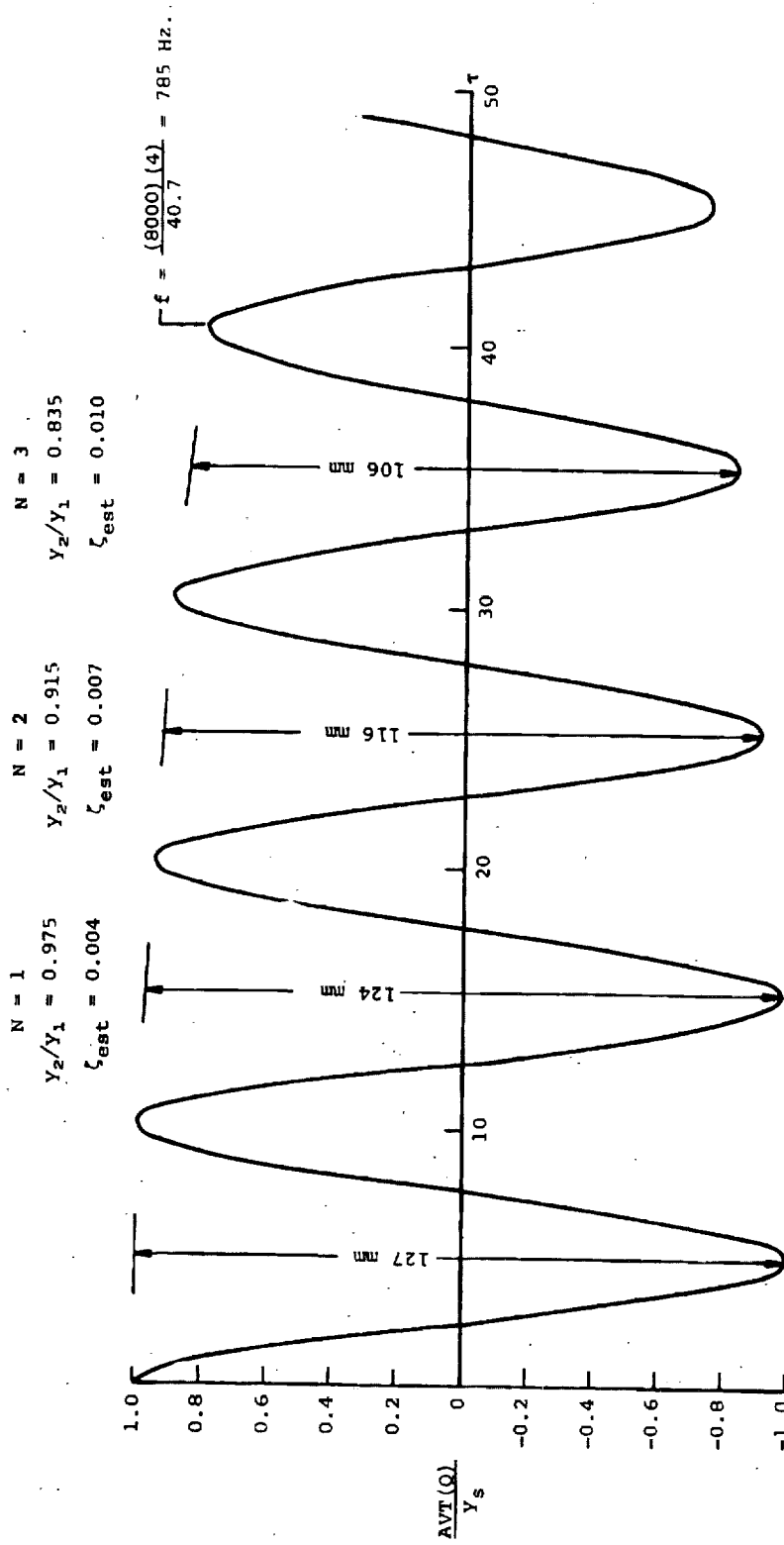
(b) Randomdec signature.

Figure 15.- Concluded.
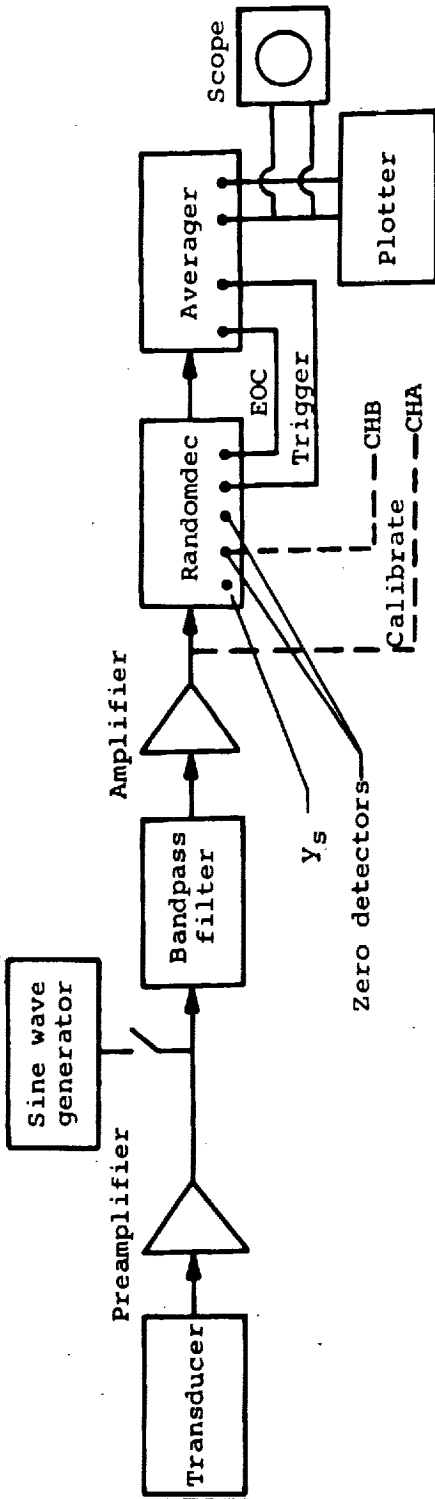
1. Select filter settings.

2. Select amplifier gain for voltage range of averager.

3. Set y_s at zero.

4. Calibrate zero detectors on oscilloscope.

   Sine wave   Channel A
   Zero det.   Channel B & ext. trigger
                D.C.

   Adjust to zero crossing as shown.

5. Select level y_s, near expected RMS.

   Number of functions, $N \approx 500$
   Sweep time, τ_{max}, 1 to 5 cycles of mode of interest
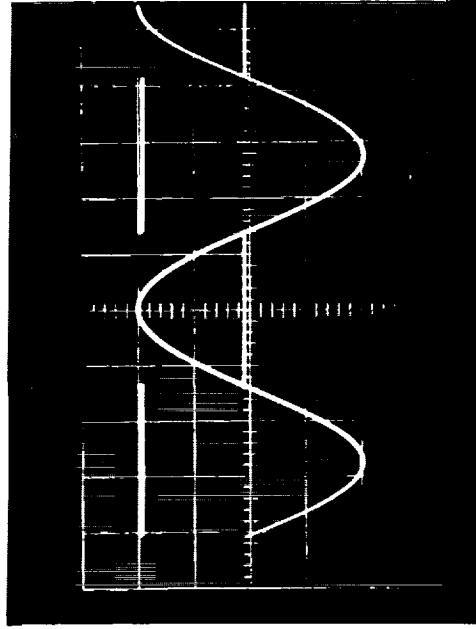
Figure 16.- Experimental setup and procedure for single channel operation.
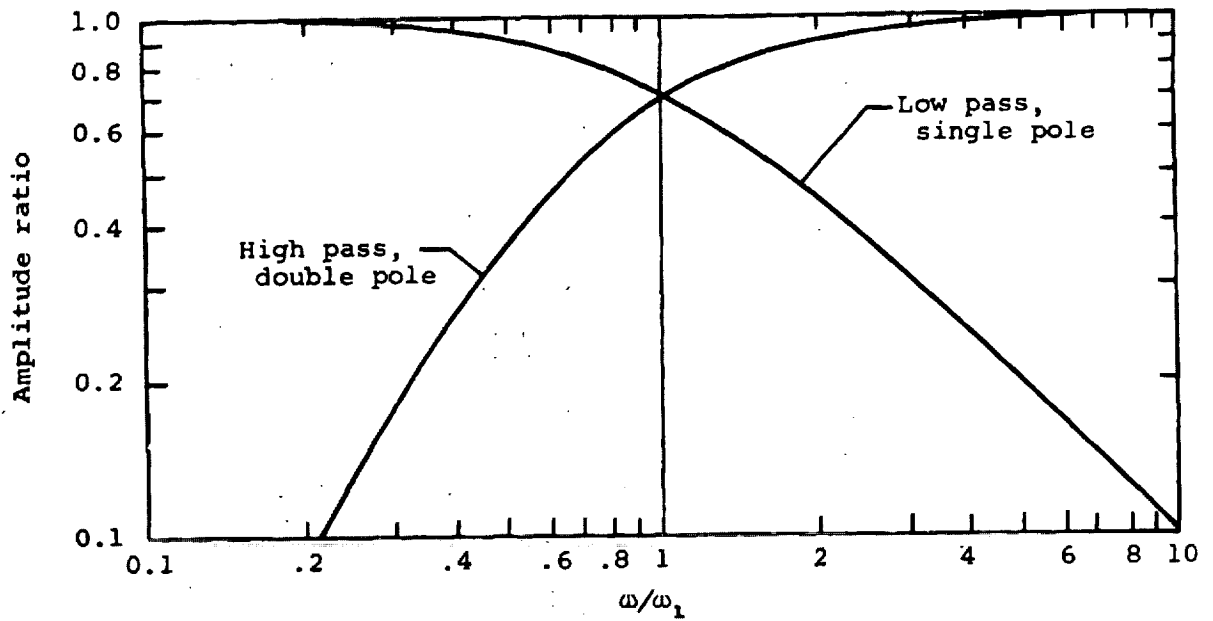
(a) Frequency response.
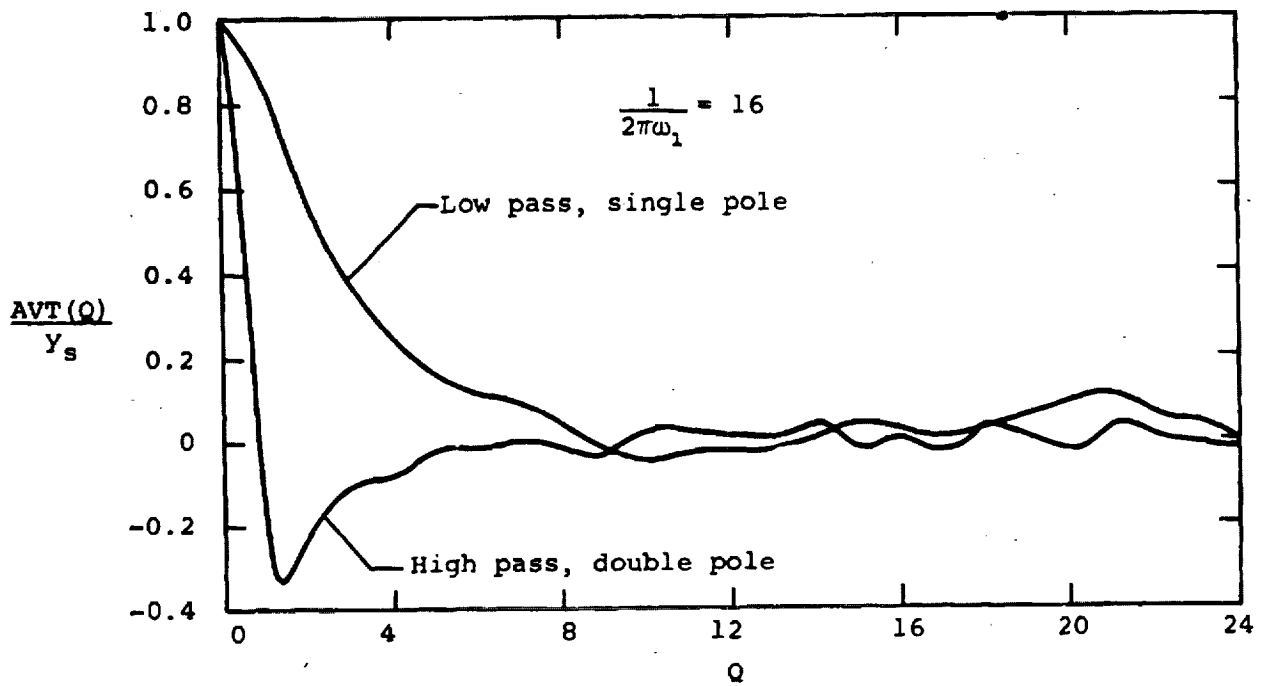
(b) Randomdec signatures.

Figure 17.- R-C filter characteristics.
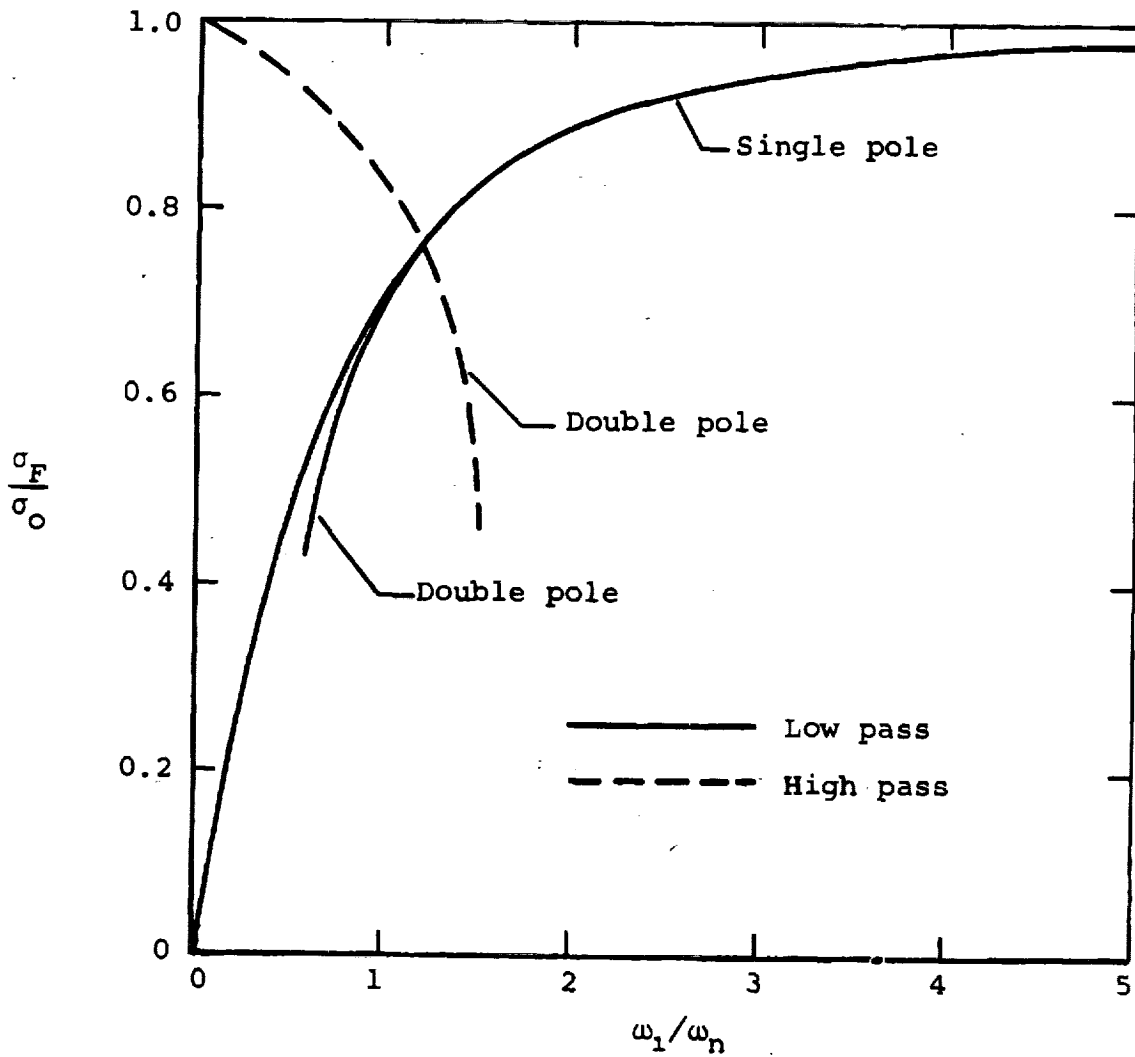
Figure 18.- Effect of filtering on RMS of output.
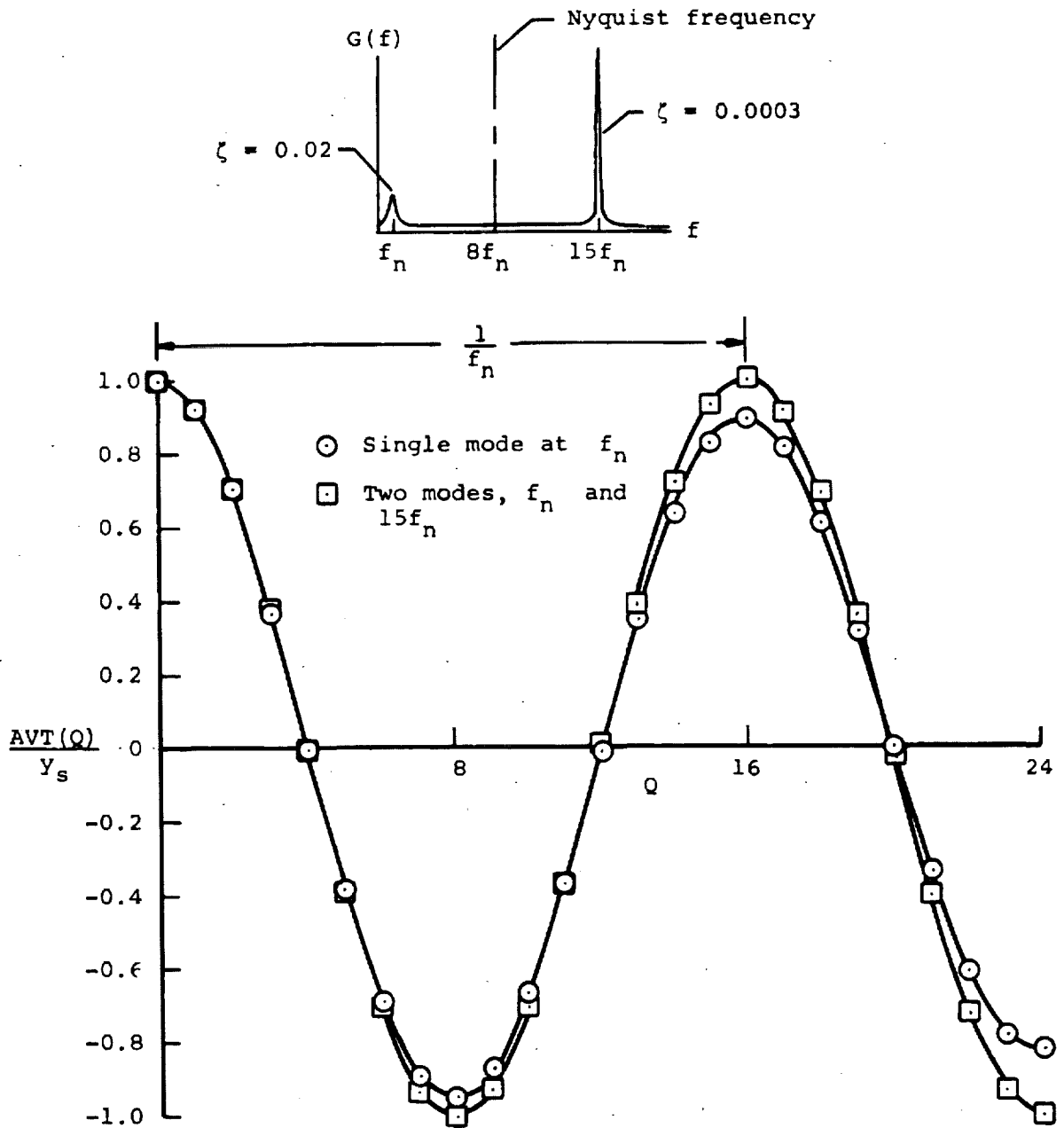
Figure 19.- Effect of aliasing on andomdec signature
for $y_s = \sigma_y$, $M = 4098$, $\zeta = 0.02$.

The y-axis is labeled "% Distortion/% Damping ratio, $c_1/c_2\zeta$" and the x-axis is labeled "ω_n/ω_1".

Autocorrelation

$$\frac{2}{\omega_1/\omega_n\left[1 + (\omega_1/\omega_n)^2\right]}$$
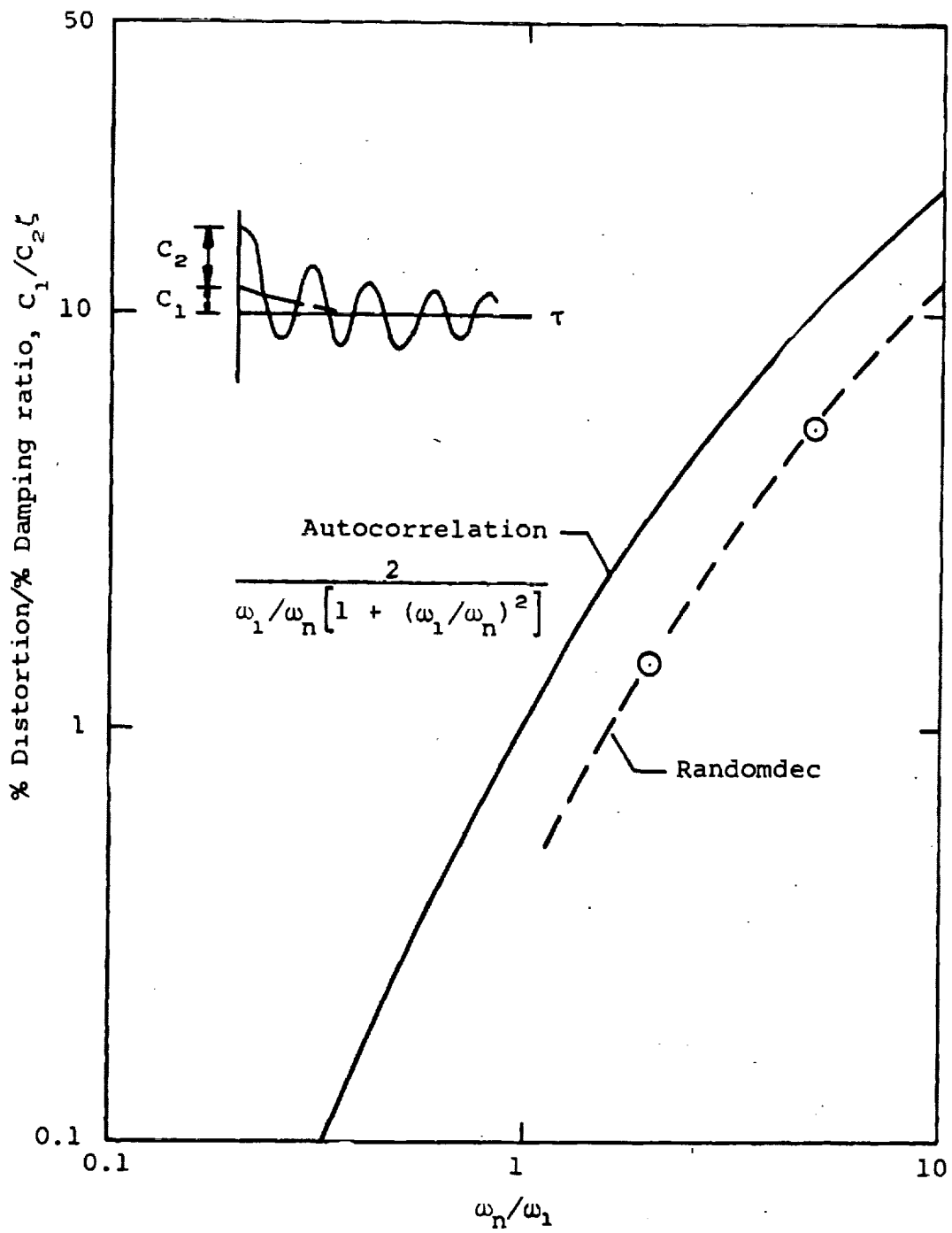
Randomdec

Figure 20.- Comparison of distortion effect of isotropic turbulence input spectrum on autocorrelation and Randomdec signatures.

Randomdec
Autocorrelation

Theoretical free vibration

Autocorrelation only shown for this range of

$\dfrac{AVT(Q)}{y_s}$

1.0 0.8 0.6 0.4 0.2 0 -0.2 -0.4 -0.6 -0.8 -1.0

10 20 30 40 50 60 70 80 90
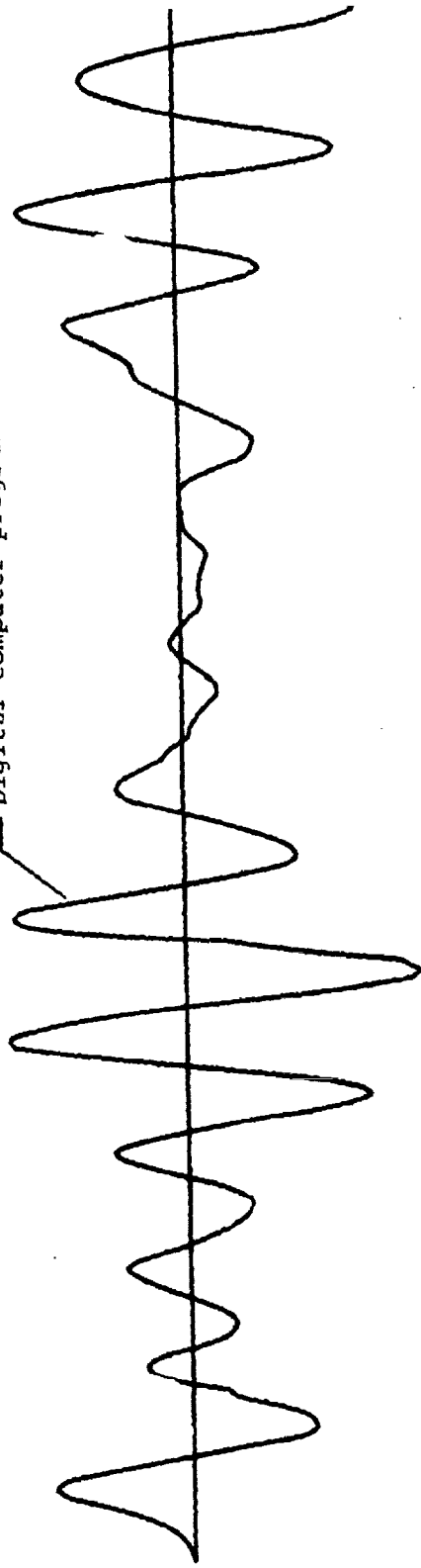
Figure 22.- Typical narrow-band random time histories.

Digital computer program

Wind-tunnel model
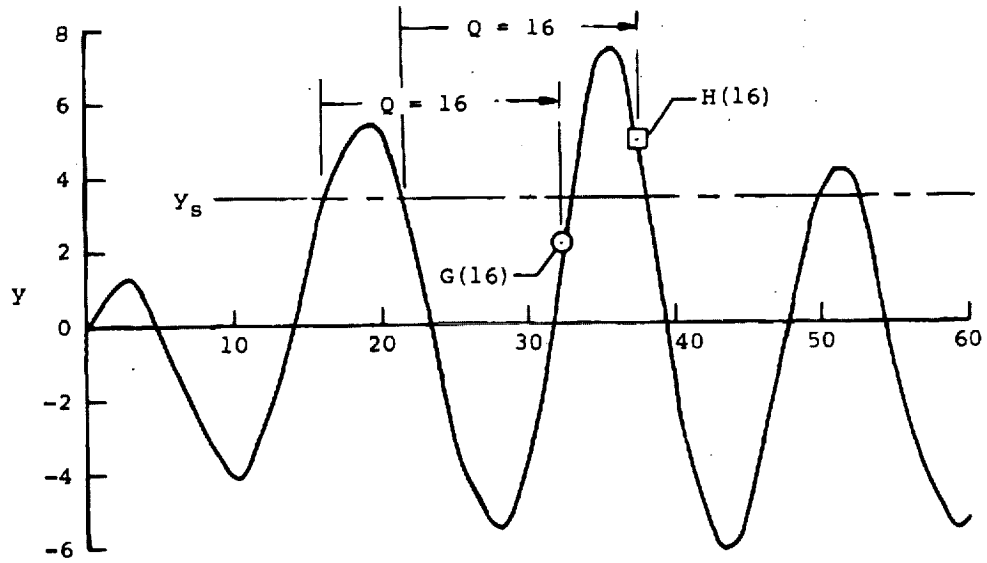
(a) Part of time history.
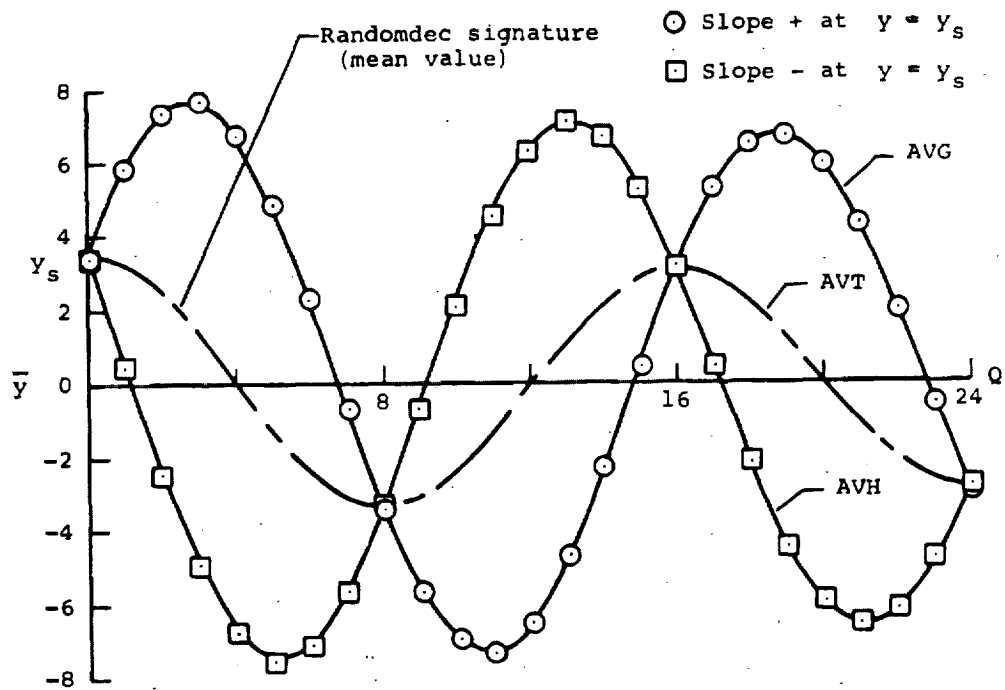
(b) Average of 222 segments of time history
with initial value equal to Y_s.

Figure 23.- Plot of computer program output
($\zeta = 0.02$, unfiltered, M = 4098).
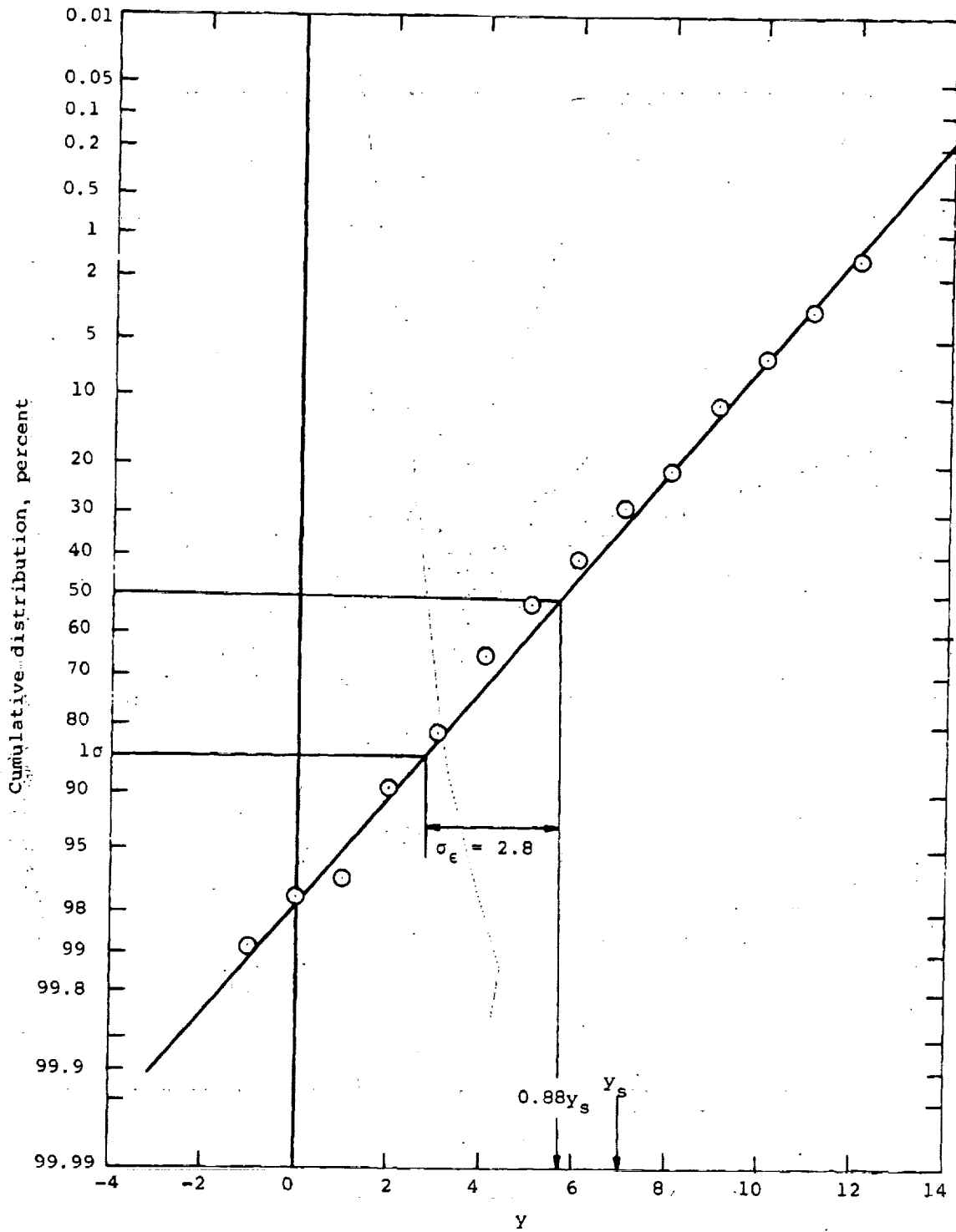
Figure 24.- Cumulative distribution of G(16) and H(16) values
for $Y_s = \sigma_y$ plotted on normal-probability paper (K = 96).
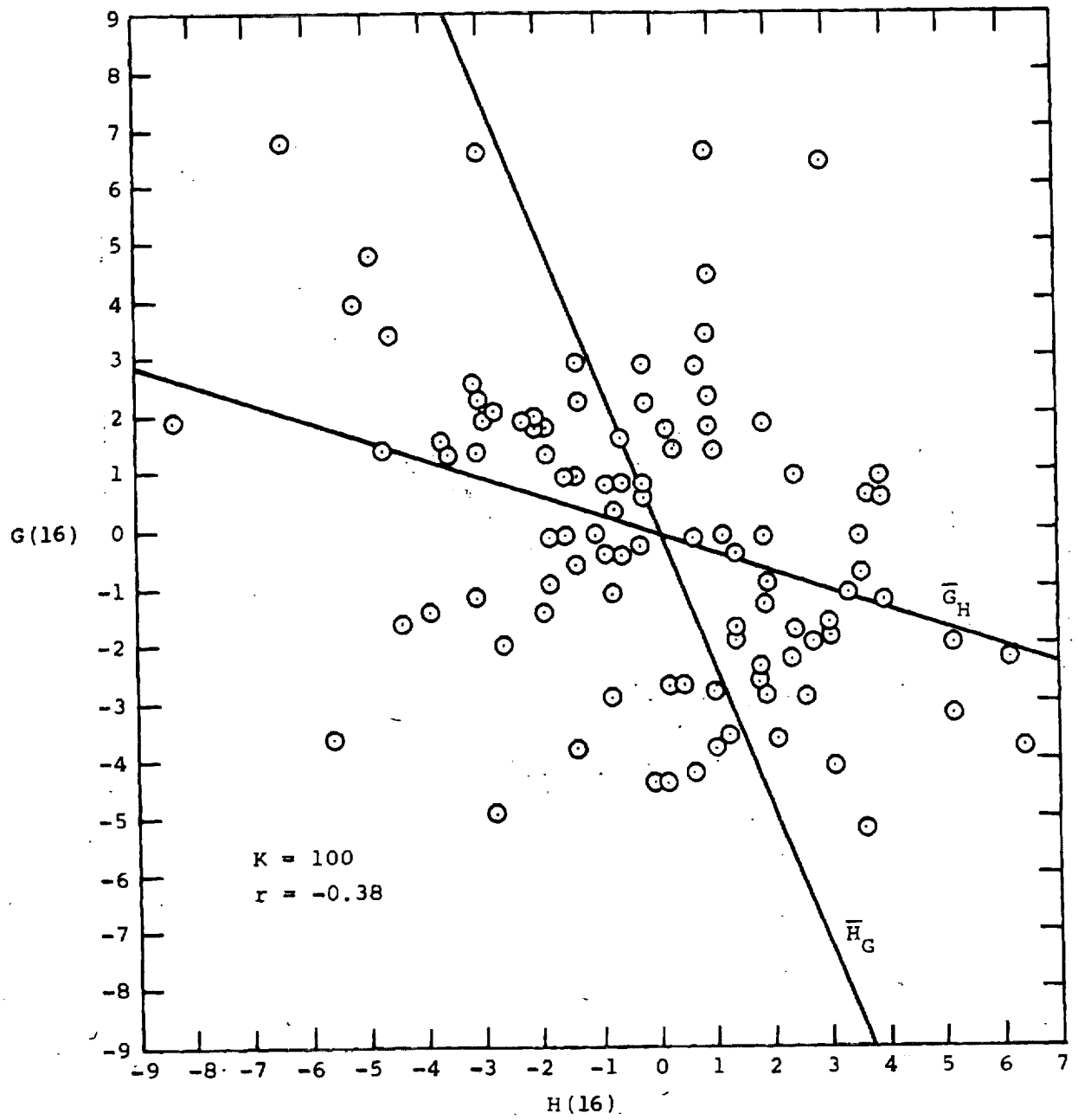
Figure 25.– Correlation of + slope values with
– slope values at $\tau = P$.

(a) $y_s = 0$.
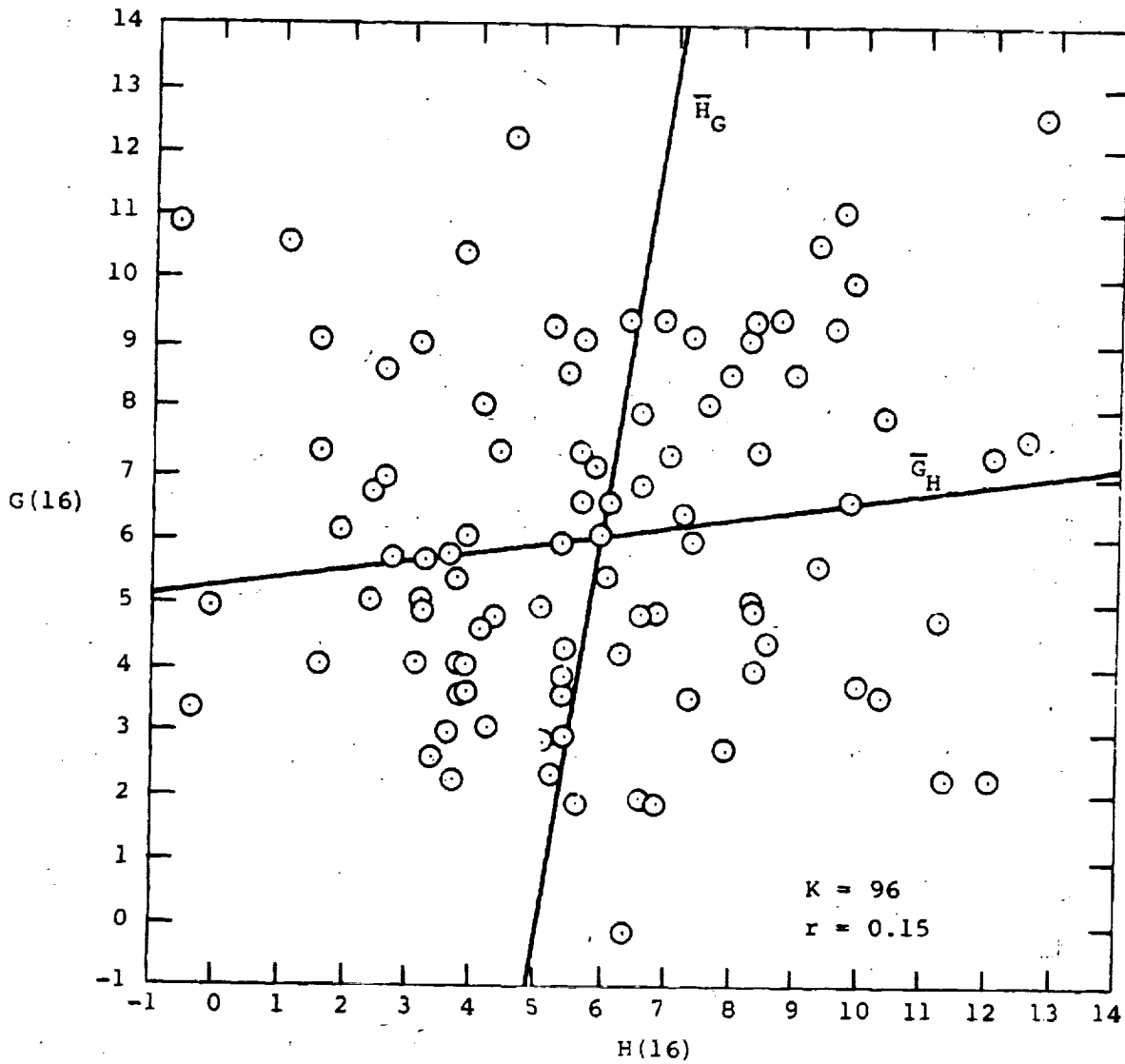
(b) $y_s = \sigma_y$.

Figure 25.- Continued.
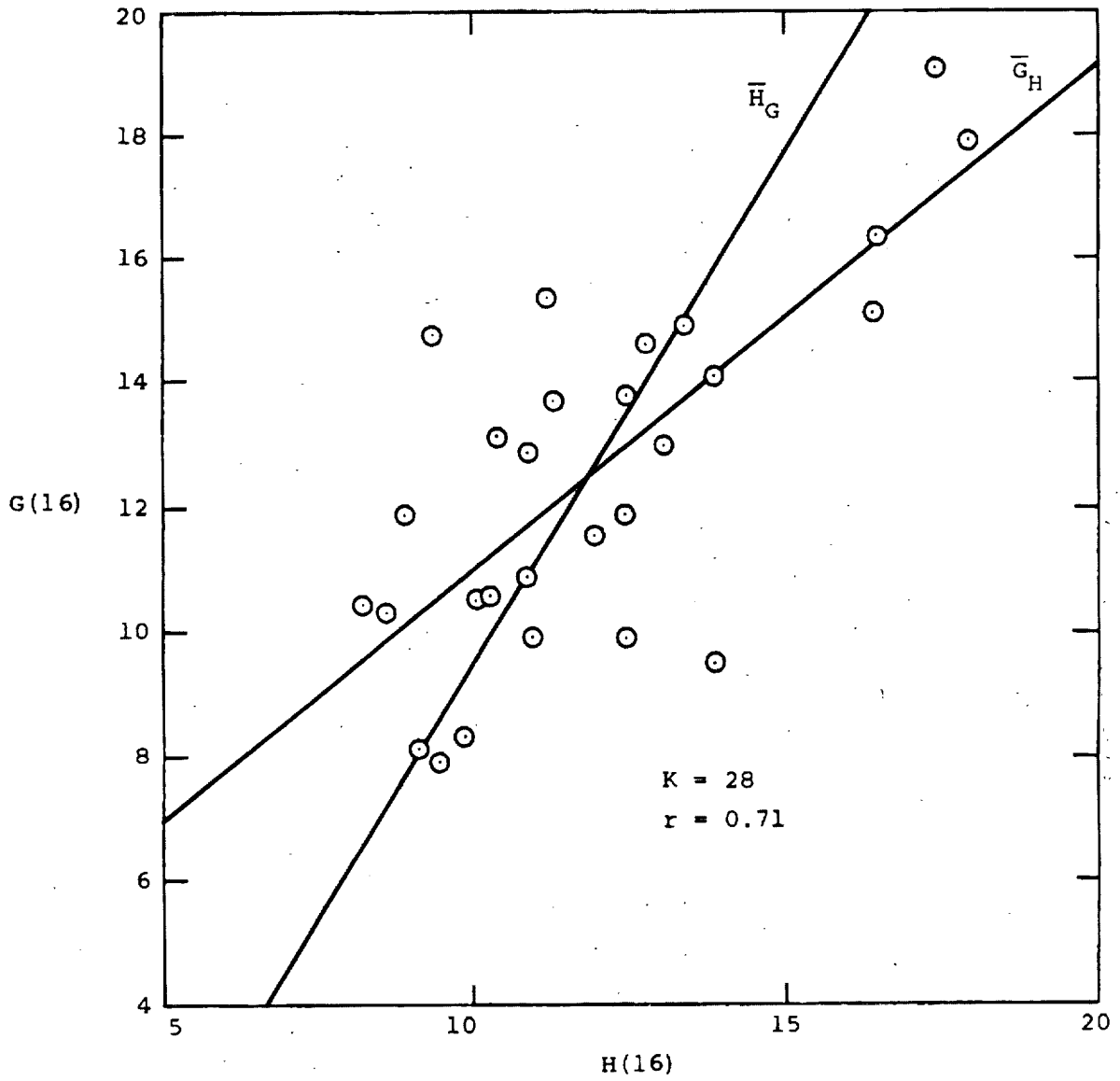
(c) $Y_s = 2\sigma_y$.

Figure 25.- Concluded.
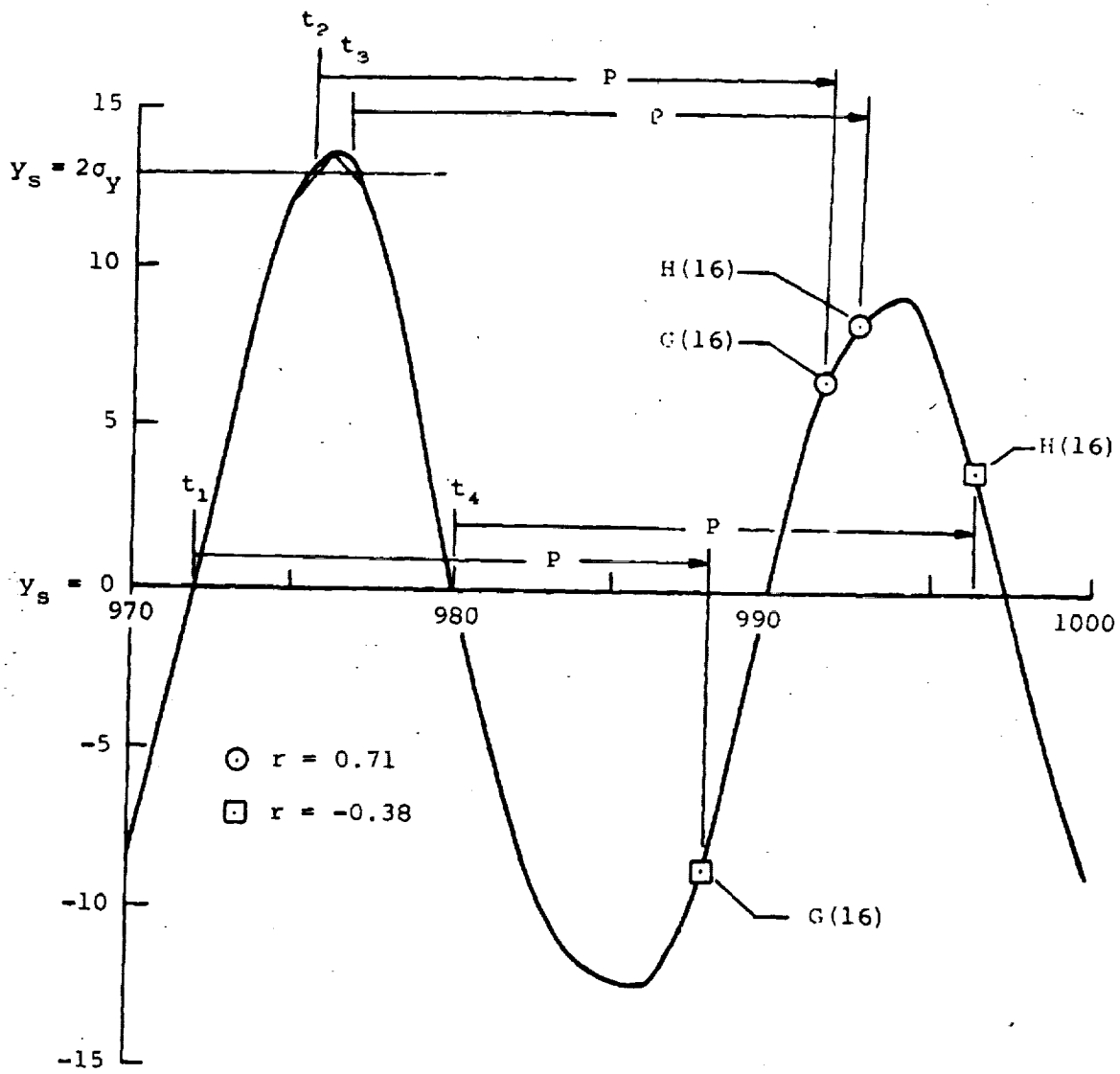
Figure 26.– Effect of selection level near a peak and
at zero for a lag of one period ($\zeta = 0.02$).
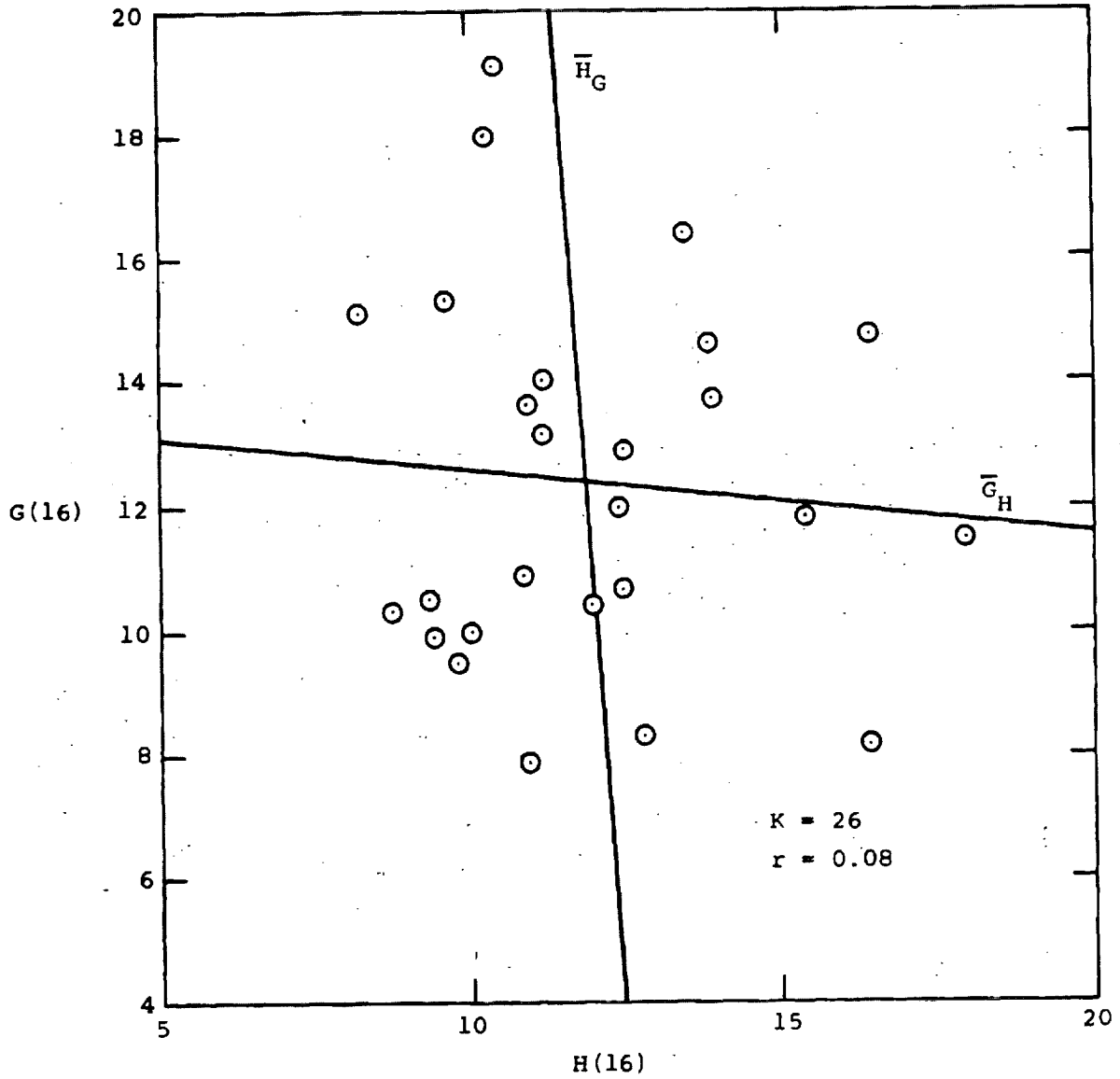
Figure 27.— Correlation of randomdec at 1P with starting
points of a plus and a minus slope on adjacent
peaks $(y_s = 2\sigma_y)$.
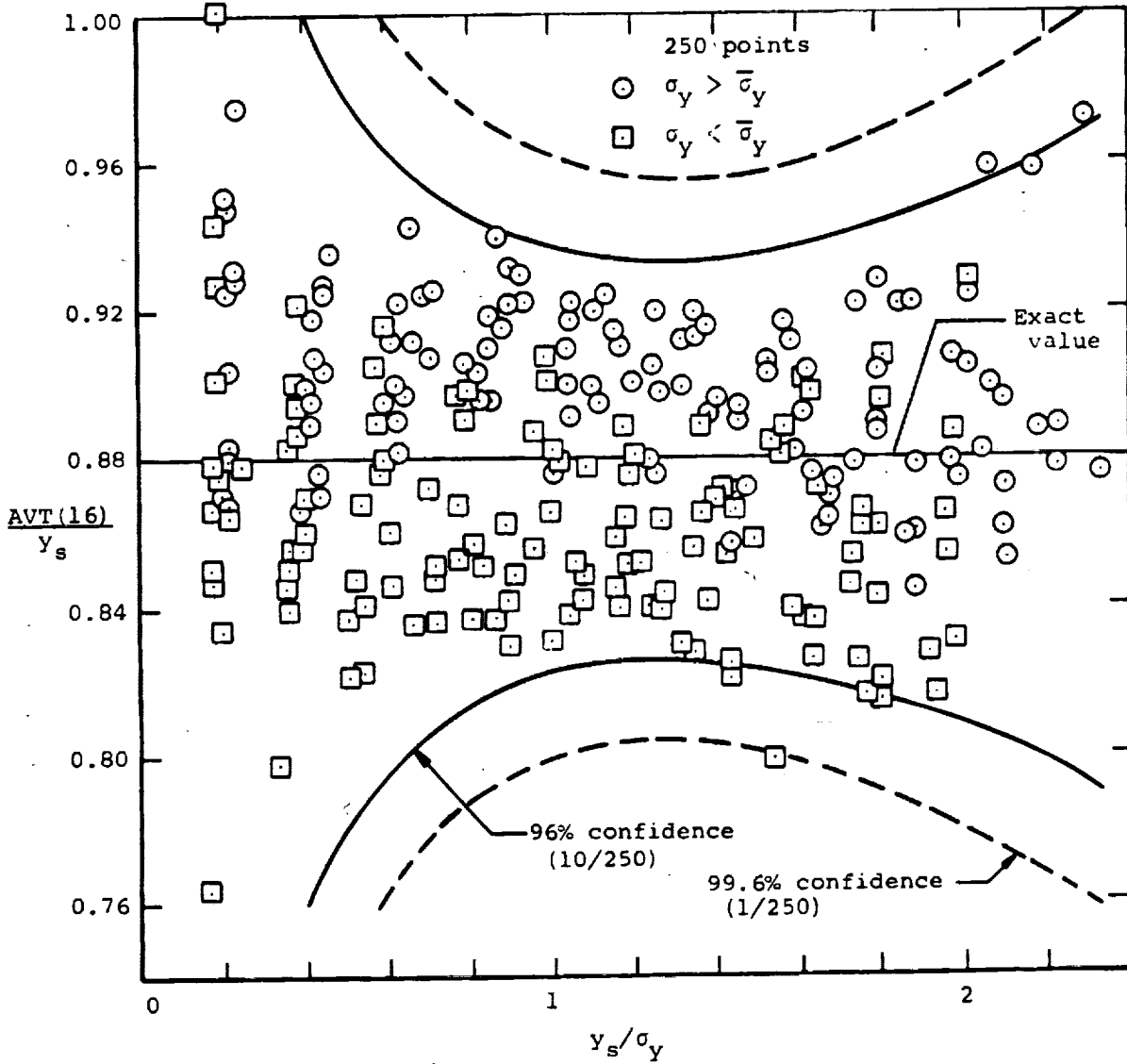
Figure 28.— Hypothesis that random decrement in the limit
gives exactly the free vibration decay value at a lag of
one period (P = Q = 16, ⌐ = 0.02, M = 4098).
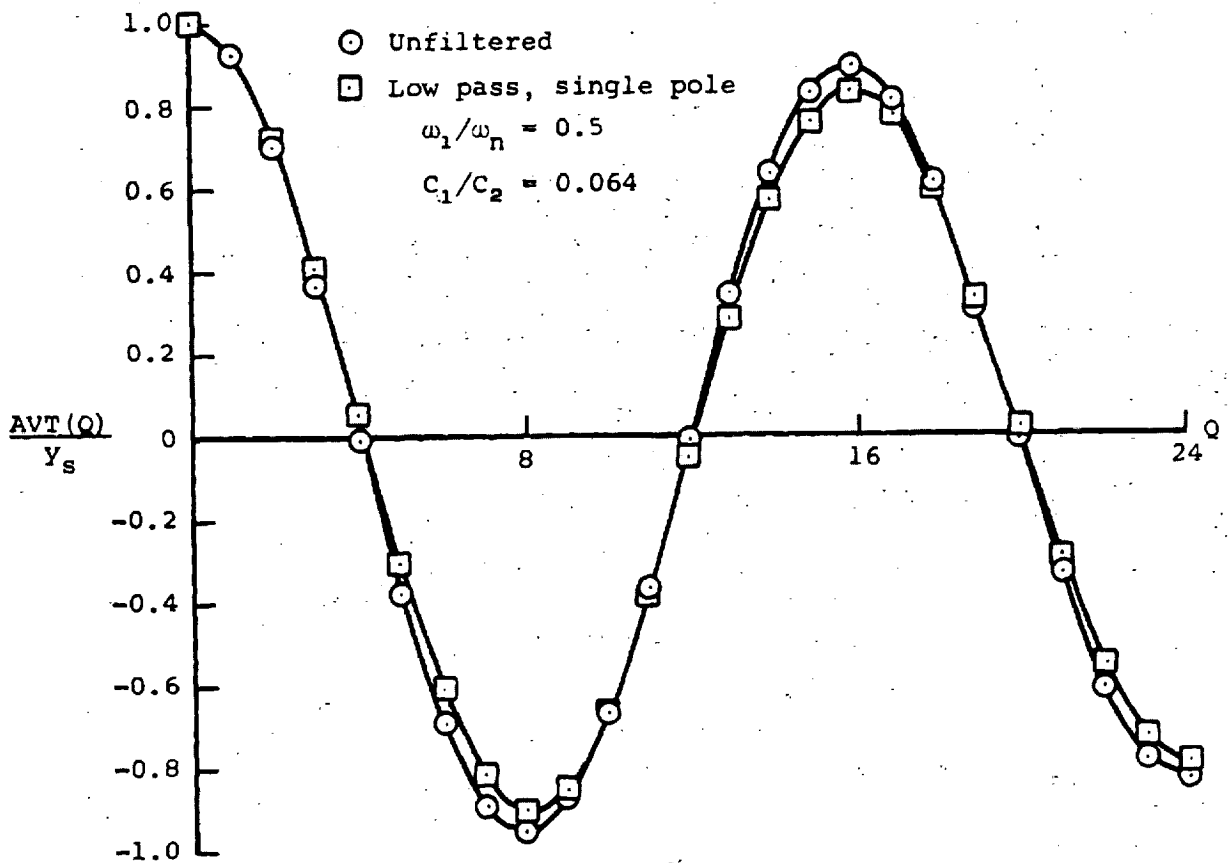
Figure 29.- Effect of low-pass R-C filter on randomdec signature for $y_s = \sigma_y$ ($\zeta = 0.02$, M = 4098).
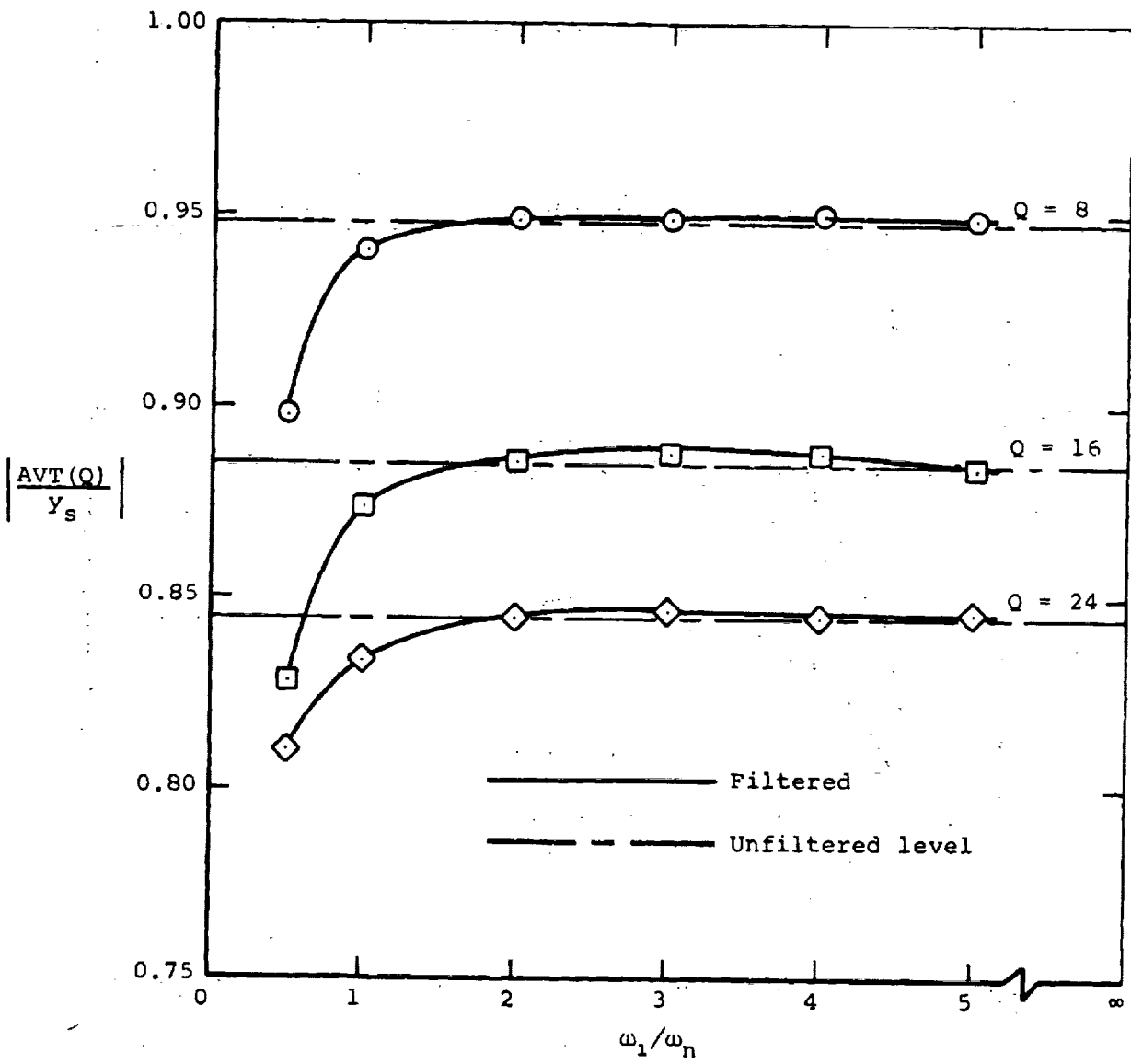
(a) Low-pass, single pole.

Figure 30.- Distortion of signature at 1/2, 1, and 1 1/2-period points due to R-C filters (M = 4098, ζ = 0.02).
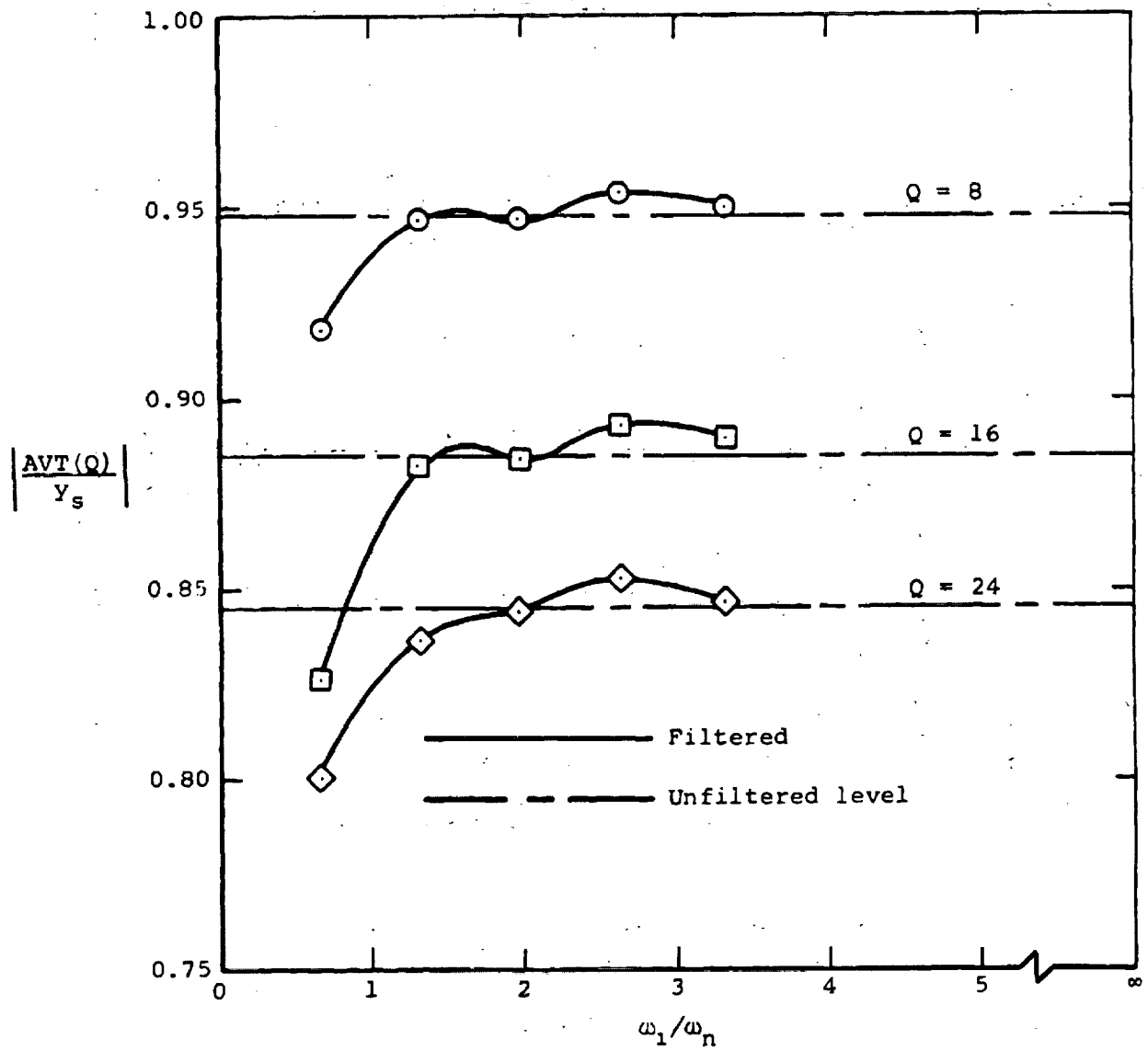
(b) Low-pass, double pole.

Figure 30.- Continued.

70
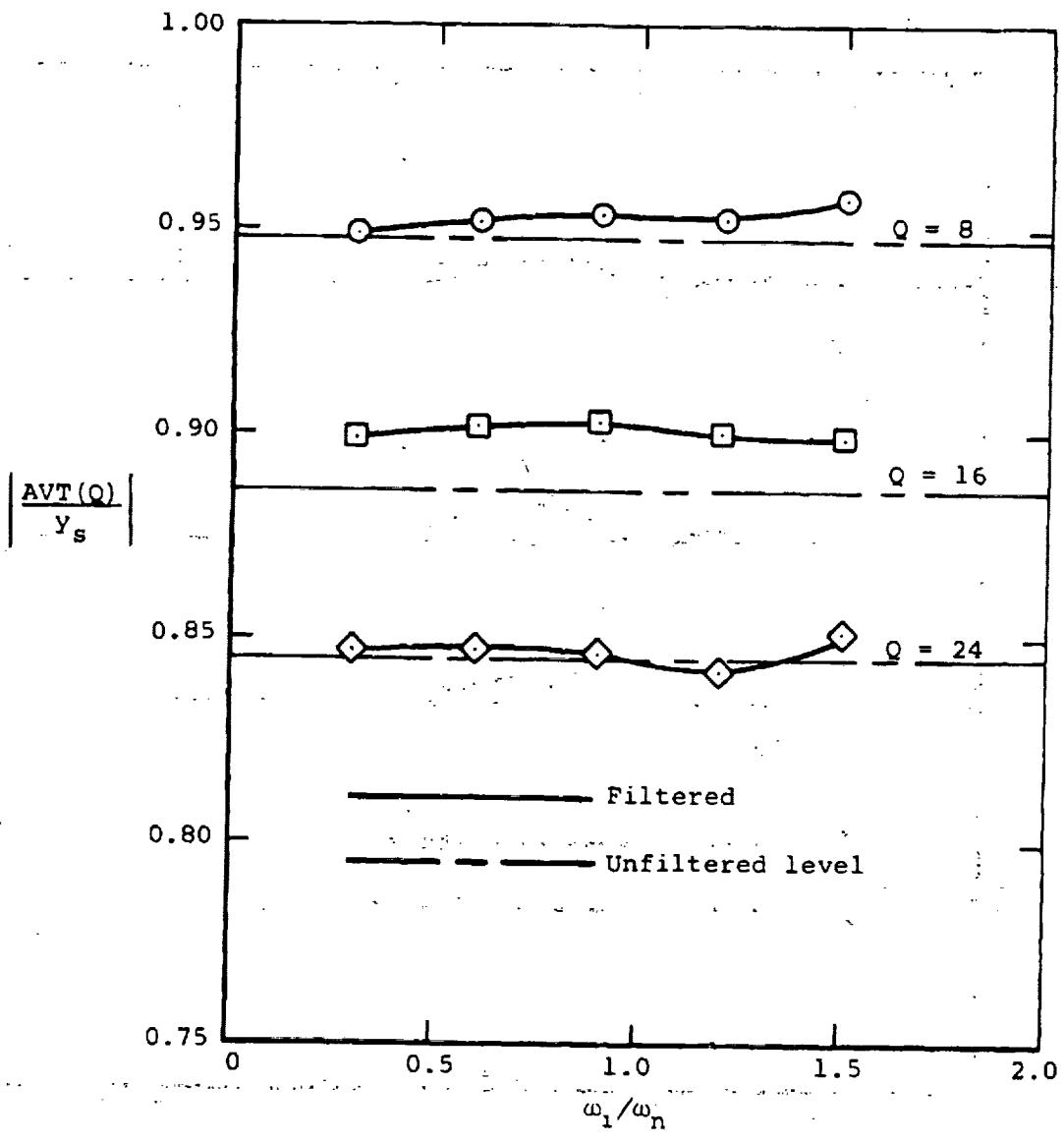
(c) High-pass, double pole.

Figure 30.- Concluded.
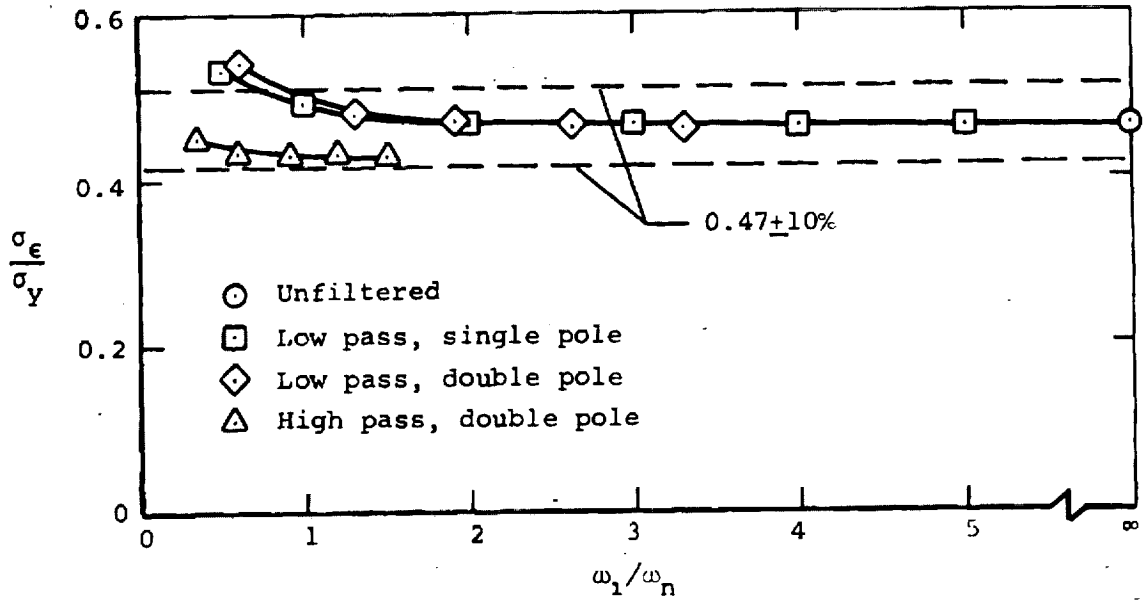
(a) Effect of filtering on σ_ϵ/σ_y ratio at constant damping ratio of $\zeta = 0.02$.
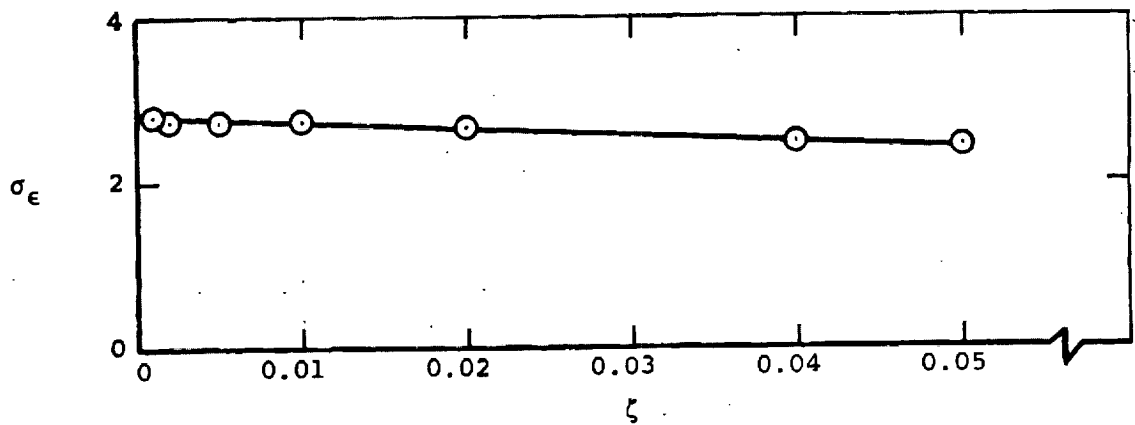
(b) Effect of damping ratio on σ_ϵ with no filtering and σ_r constant.

Figure 31.- Variation of standard deviation of Randomdec with filtering and damping ratio.
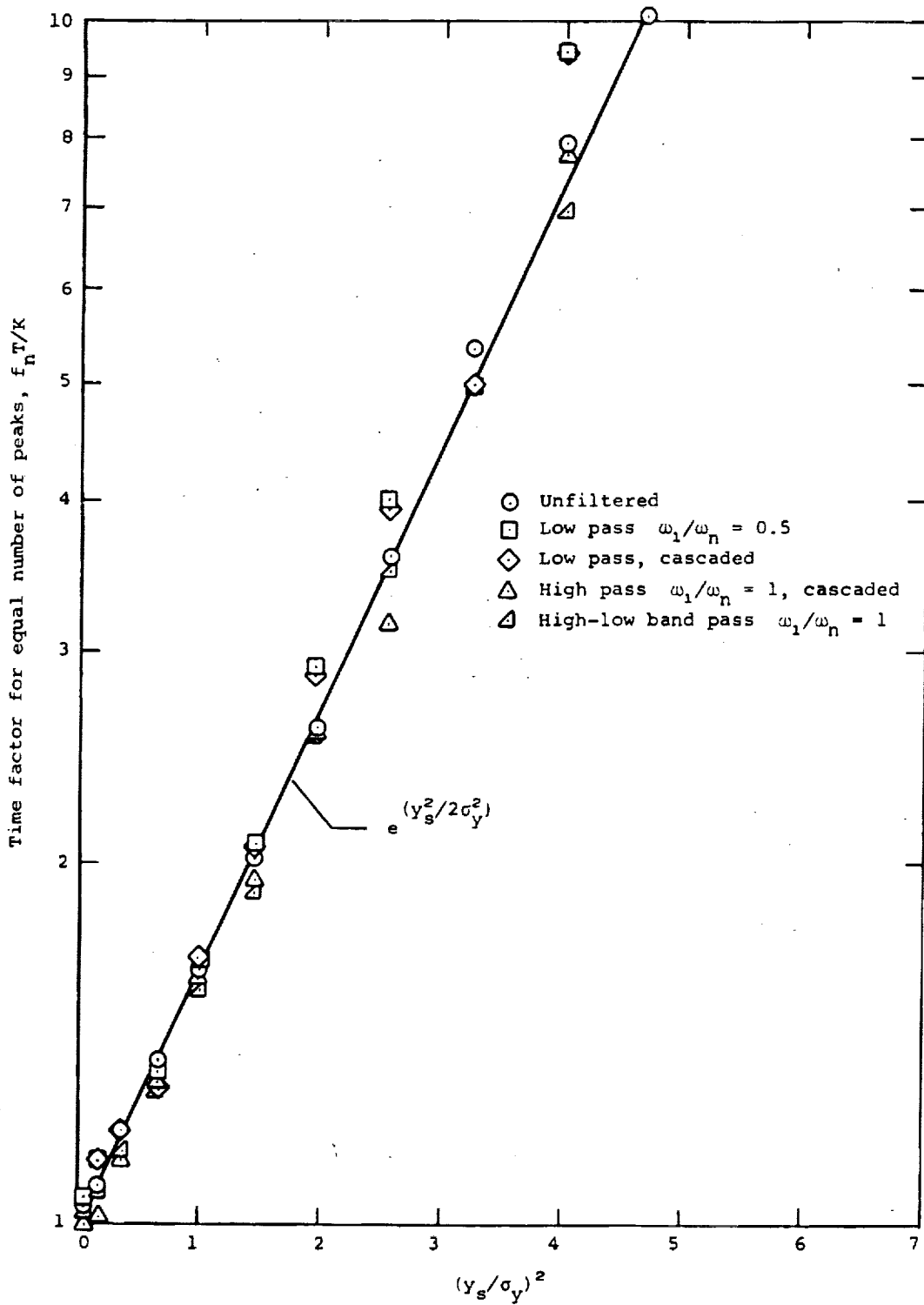
Figure 32.- Measured and predicted time factors.
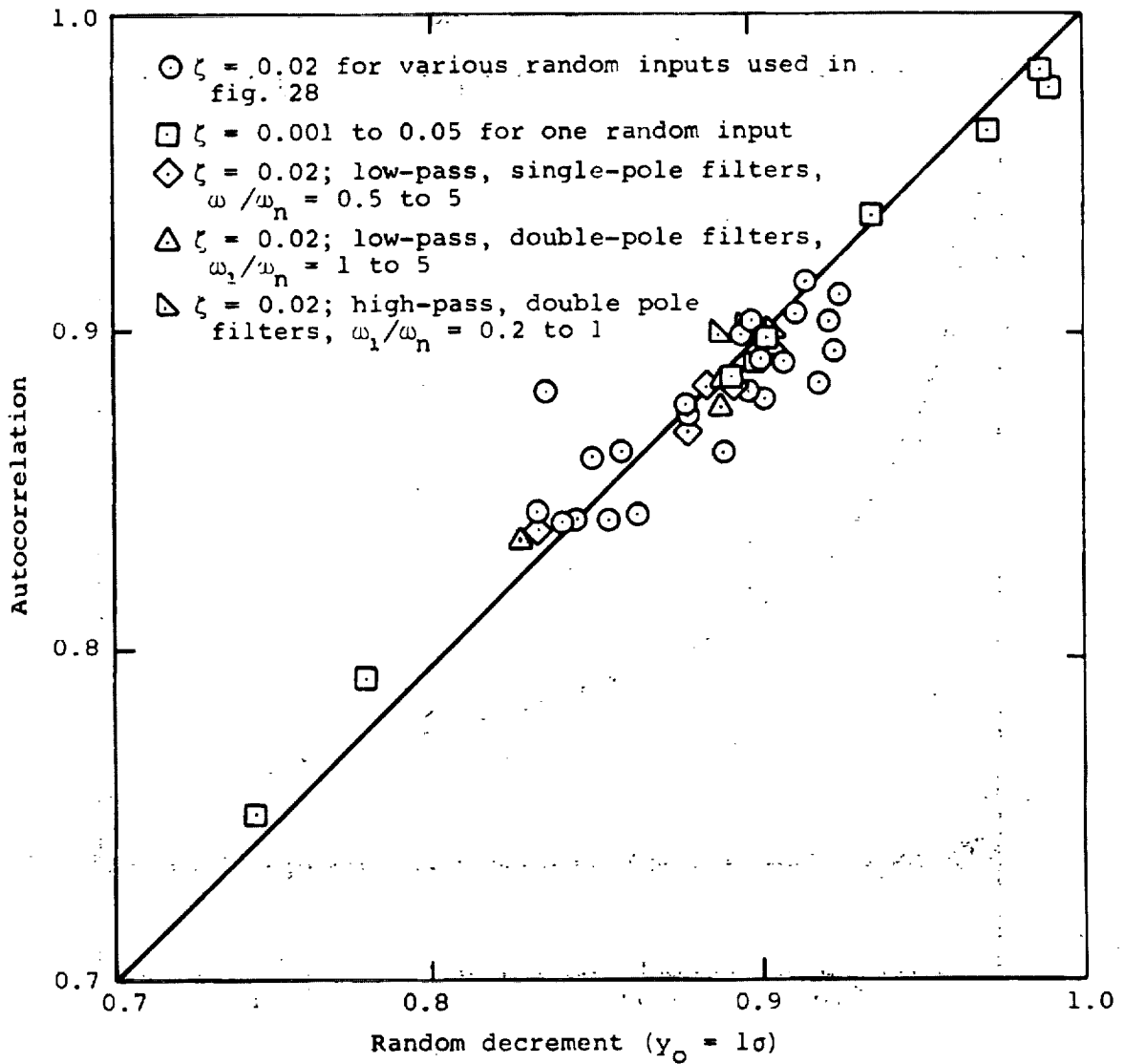
Figure 33.- Comparison of random decrement with autocorrelation
values at a time lag of one period.
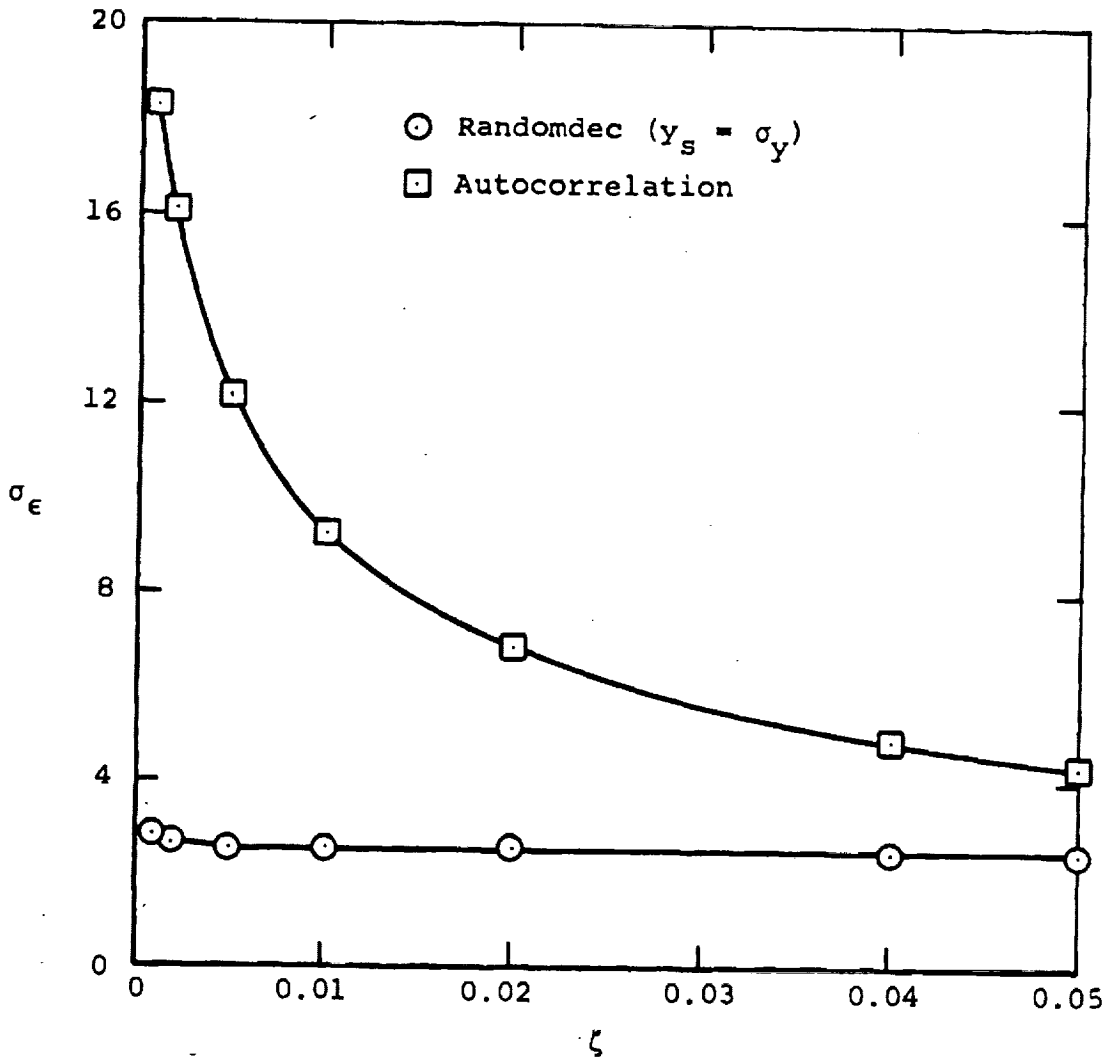
Figure 34.- Standard deviation of randomdec and autocorrelation for various damping ratios.